Helium Chemistry: Theoretical Predictions and Experimental Challenge[1]

Wolfram Koch,[†2a] Gernot Frenking,*[2b] Jürgen Gauss,[2c] Dieter Cremer,*[2c] and Jack R. Collins[2b]

Contribution from the Institut für Organische Chemie, Technische Universität Berlin, Strasse des 17, Juni 135, D-1000 Berlin 12, West Germany, the Molecular Research Institute, 701 Welch Road, Palo Alto, California 94304, and the Institut für Organische Chemie, Universität Köln, Greinstrasse 4, D-5000 Köln 41, West Germany. *Received December 22, 1986*

Abstract: Quantum mechanical investigations at the MP4(SDTQ)/6-311G(2df,2pd)//MP2/6-31G(d,p) + ZPE level of theory show that helium is capable of forming strong bonds with carbon in cations and that even a neutral molecule containing He (HeBeO) can be thermodynamically stable in its ground state. The electronic state of a binding partner is crucially important for the bond strength and bond length of the He bond. He_2C^{2+} has a rather long (1.605 Å) He–C atomic distance in its $^1A_1$ ground state, but a much shorter bond (1.170 Å) is found in the $^3B_1$ excited state. The shortest He–C bonds (1.080–1.085 Å) are found in the $\Sigma^+(4\pi)$ states of $HeCC^{2+}$, $HeCCHe^{2+}$, and $HeCC^+$. The bond dissociation energies of the dications in these electronic states yielding neutral He and a cationic fragment are predicted to be as high as 89.9 kcal/mol for $HeCC^{2+}$. Helium compounds are best understood as donor–acceptor molecules consisting of He as electron donor and the respective acceptor fragment. Strong helium bonds are formed when a binding partner (acceptor) provides low-lying empty σ orbitals (σ-holes). Electronegative elements such as fluorine or oxygen are not suitable for binding He due to their highly filled valence shells. More promising candidates should provide empty orbitals which are still capable of attracting the low-lying 1s electrons of the poor electron donor He. The stability of HeBeO is confirmed by CASSCF calculations with a 6-31G(d,p) basis set and an active space of all 14 electrons in 11 orbitals. The structures and energies of the helium compounds are rationalized by molecular orbital arguments and by analysis of the electron density and its associated Laplace field. The strongly bound helium ions are characterized by covalent semipolar He–C bonds, whereas the weaker bonds in some structures are caused by electrostatic interactions between closed-shell systems. The impact of our study on experiment, especially interstellar chemistry, is discussed.

1. Introduction

The reluctance of the noble gases to form chemical bonds is a challenge for the inventive chemist. For many years noble-gas chemistry had been considered as nonexistent. In 1962, N. Bartlett[3] synthesized the first neutral molecule containing the heavy noble gas xenon, taking advantage of the fact that the ionization energy of xenon is lower than for molecular oxygen. In a similar fashion neutral molecules containing krypton and radon have been prepared.[4] For the lighter elements argon, neon, and helium only ionic species seem to be candidates to bind with them chemically since the polarizabilities of these noble-gas elements are lower and their ionization energies are much higher. Since the rare gases contain completely filled valence shells, only electron withdrawal can lead to chemical binding. Helium has the highest ionization energy of all chemical elements (24.587 eV)[5] and thus is the most difficult element to bind. In fact, the energy needed to remove one electron from a helium atom to produce He^+ is even slightly higher than the second ionization energy of carbon (24.383 eV).[5] Considering electronegativities, no chemical element should be capable of forming a chemical bond with helium.

One possibility to attract electrons from He is a "brute-force" approach employing highly charged cations as binding partners. The electron attraction of doubly charged particles may be strong enough to polarize helium sufficiently to form a chemical bond, but dications encounter strong charge repulsion. However, in spite of the inherent Coulomb repulsion, doubly charged cations may have strong bonds. In some cases bonds are much stronger in a doubly charged molecule than in the respective neutral counterpart.[6,7] For example, the ylid bonds in the so-called ylid dications often have a substantial barrier for the dissociation reaction, while the respective neutral ylid structures are barely bound.[6] The strength of these bonds may be considered as and explained by donor–acceptor interaction between a neutral donor and dicationic acceptor species.[7]

Removing electrons from a diatomic molecule AB may lead to a shorter and stronger bond between A and B, or it may actually introduce a bond which is absent for the neutral system. A prominent example is He_2^{2+} which was predicted by Pauling as early as 1933[8] to exist as a metastable molecule, i.e., a molecule which is thermodynamically unstable toward dissociation, but has a sufficiently high barrier to be prevented from spontaneous dissociation. He_2^{2+} has recently been observed by charge-stripping mass spectrometry.[9]

The effect of nuclear charge on binding energies in hydrogen-like molecules has quantitatively been studied by Dunitz and Ha,[10] and it was found that "a bond may be strengthened by effective positive charges on adjacent nuclei provided the charges are not too large".[10] For molecules other than hydrogen, several factors will be effective; e.g., the type of orbital (bonding or antibonding) and the difference in electronegativity χ between A and B. The Coulomb repulsion between positively charged atoms A and B in dications AB^{2+} will decrease with increasing difference between χ_A and χ_B, while at the same time the importance of charge-polarization terms $(A^{2+}–B)$[11] will increase. Thus, the bond-strengthening effect of removing electrons from

[†] Present address: IBM Research Center, San Jose, CA 95193.

(1) Parts of this study have been reported in preliminary communications: (a) Koch, W.; Frenking, G. *J. Chem. Soc., Chem. Commun.* **1986**, 1095. (b) Koch, W.; Frenking, G. *Int. J. Mass Spectrom. Ion Proc.* **1986**, *74*, 133. (c) Koch, W.; Collins, J. R.; Frenking, G. *Chem. Phys. Lett.* **1986**, *132*, 330.

(2) (a) Technische Universität Berlin. (b) Molecular Research Institute. (c) Universität Köln.

(3) Bartlett, N. *Proc. Chem. Soc.* **1962**, 218.

(4) (a) Bartlett, N. *The Chemistry of the Noble Gases*; Elsevier: Amsterdam, 1971. (b) Hawkins, D. T.; Falconer, W. E.; Bartlett, N. *Noble Gas Compounds*; Plenum Press: New York, 1978.

(5) *Handbook of Chemistry and Physics*, 65th ed.; CRC Press: Boca Raton, FL, 1984–1985.

(6) (a) Radom, L.; Bouma, W. J.; Nobes, R. H.; Yates, B. F. *Pure Appl. Chem.* **1984**, *56*, 1831. (b) Yates, B. F.; Bouma, W. J.; Radom, L. *J. Am. Chem. Soc.* **1986**, *108*, 6545.

(7) Koch, W.; Frenking, G.; Gauss, J.; Cremer, D. *J. Am. Chem. Soc.* **1986**, *108*, 5808.

(8) Pauling, L. *J. Chem. Phys.* **1933**, *1*, 56.

(9) (a) Guilhaus, M.; Brenton, A. G.; Beynon, J. H.; Rabrenovic, M.; Schleyer, P. v. R. *J. Phys. B* **1984**, *17*, 605. (b) Guilhaus, M.; Brenton, A. G.; Beynon, J. H.; Rabrenovic, M.; Schleyer, P. v. R. *J. Chem. Soc., Chem. Commun.* **1985**, 210.

(10) Dunitz, J. D.; Ha, T. K. *J. Chem. Soc., Chem. Commun.* **1972**, *568*.

(11) Wetmore, R. W.; Le Roy, R. J.; Boyd, R. K. *J. Phys. Chem.* **1984**, *88*, 6318.

0002-7863/87/1509-5917$01.50/0

a diatomic molecule AB may be expected to be strongest when χ_A and χ_B differ most, and when the electrons are removed from antibonding orbitals. This idea is supported by the calculated bond distances for CF^{n+} which were found at the MP2/6-31G(d) level as 1.291, 1.173, 1.146, and 1.182 Å for n = 0, 1, 2, and 3, respectively.[12] A subsequent CASSCF investigation on CNe^{n+} showed deep minima for the $^1\Sigma^+$ ground state and $^3\pi$ excited state of CNe^{2+} with atomic distances of 1.561 and 1.418 Å, respectively.[13] Thus, carbon may form a chemical bond to neon in metastable dicationic species.

Helium is less polarizable than neon, but there is a distinct difference to the other noble gas elements: Helium has no p orbitals in the valence space. Thus, orbital interaction of electrons occupying π orbitals in a molecule with helium located in the σ-space is not possible for symmetry reasons. Cooper and Wilson[14] found in their SCF studies on noble gas molecular ions that helium forms shorter bonds in unsaturated ions than in saturated molecules. We found that the geometries and stabilities of helium compounds are strongly affected by the electronic structure of the molecule. A comparison of the calculated geometries and stabilities with the results of the electron density analysis suggests an intriguing possibility for binding helium chemically. Donor–acceptor interaction, which has successfully been employed to explain the peculiar structures of dications,[7] proved to be very useful to rationalize and to design helium compounds. The stability of He-containing dications, monocations, and neutral species can be explained by donor–acceptor interactions between He as electron donor and the respective fragment as electron acceptor. It is the electronic state of the binding partner, rather than the electronic charge or electronegativity, which determines the bond strength of the He–X bond.

Noble-gas chemistry in the past has been characterized by searching for electronegative elements or groups which have sufficient polarizing strength to attract electronic charge from the inert elements. As a consequence, stable bonds are found only for Kr, Xe, and Ra to F, Cl, O, and N.[4] We found that for helium a different strategy in searching for binding partners should be employed: If a first-row atom or molecule has low-lying empty σ orbitals ("σ-holes"), while p(π) orbitals are occupied, the polarizing attraction for helium is sufficient to form strong bonds in cations, and He may even form neutral molecules which are thermodynamically stable in their ground states. Rather than atoms such as fluorine or oxygen which are very electronegative but have many electrons in the valence space, C-, B-, and Be-containing acceptor molecules are more suitable binding partners due to the presence of low-lying empty orbitals.

Previous theoretical work on molecules with chemical bonds between helium and first-row elements other than neon is very rare. With two exceptions, only ionic molecules have been investigated. Fereday and Sinha published results of their pen-and-paper calculations on HeO, HeO_2, He_2O, and HeOF and predicted that HeOF should be a stable species.[15] Kaufman and Sachs investigated HeLiH at the Hartree–Fock level and found it to be bound by 0.08 eV.[16] Cooper and Wilson performed SCF studies on singly and multiply charged diatomic ions HeX^{n+} (X = C, N, O) and some polyatomic species such as $HeCN^+$, $HeCO^{2+}$, $HeCCH^+$, and $HeNN^{2+}$.[14] $HeCN^+$ and $NeCN^+$ have been investigated theoretically by Wilson and Green.[17] Harrison et al. reported SCF results for He_2Be^{2+} which was predicted to be stable against dissociation into $HeBe^{2+}$ and He.[18] Very recently, Wong et al.[19] reported ab initio results of singly and multiply charged cations CHe_n^{n+} (n = 1, 2, 3, 4). He_nBe^{2+} clusters and CHe_4^{4+} have been reported in an overview on multiply charged cations by Schleyer.[20] Besides this, only diatomic ions have been studied. Harrison et al.[21] reported the potential curves of HeC^{n+}, and Liebman and Allen[22] studied HeN^+, HeB^+, and HeF^+. Theoretical studies on $HeBe^{2+}$ have been reported by several groups at the SCF[18,23] and CASSCF level.[24] SCF results were also reported for $HeLi^+$ by Krauss et al.[25] and Catlow et al.[26] HeO^+ was studied by Augustin et al.,[27] by using a minimum basis set and configuration interaction including all single and double excitations.

Experimentally even less is known. The easiest way to obtain helium-containing cations should be by using tritiated compounds as precursors since He^+ is formed as the result of radioactive decay of tritium. Although the products of the β-decay of a number of tritiated hydrocarbons have been investigated, only spurious amounts of helium ions have been detected.[28] For example, CH_3He^+ was observed by Snell and Pleasonton[29] as the product of the β-decay of CH_3T with less than 0.1% yield. Inspired by our predictions,[1b] Young and Coggiola[30] recently detected an ion in a mass spectrometer containing a carbon–helium bond formed by interaction of He^+ with graphite.

In this study we report our theoretical results on the structures, stabilities, and bonding of small doubly and singly charged cations containing helium such as He_2C^{2+}, $HeCCHe^{2+}$, $HeCC^{2+}$, HeC^{2+}, $HeCCH^+$, $HeCC^+$, and HeC^+. We present data on the effect of the heteroatoms nitrogen and oxygen on the structures and energies, i.e., He_2X^{2+}, $HeXXHe^{2+}$, and HeX^+ (X = N, O). Furthermore, we report theoretical results for the neutral molecules HeBBHe, HeCBH, HeBCH, HeBN, and HeBeO. The results provide insight in the structural features of molecules containing chemically bound helium. In particular, we address the following questions: (a) What kind of molecules form chemical bonds to helium, and what are the structural conditions under which a helium bond may be anticipated? (b) How short may the equilibrium atomic distance between carbon and helium become in a molecule, and how does it compare with the carbon–hydrogen bond in the respective isoelectronic species? (c) What is the effect of replacing carbon with other first-row elements in forming bonds with He? (d) What are the stabilities of these molecules toward dissociation? (e) What is the nature of the helium bond in the investigated compounds?

We answer these questions by analyzing energies, geometries, wave functions, i.e., MOs, and the total electron density distribution utilizing techniques that have been proven very useful in the theoretical investigation of dications.[7]

2. Quantum Chemical Methods

Most of the theoretical investigations reported here have been performed by using the CRAY version of GAUSSIAN82.[31] Optimized geometries are reported resulting from two levels of theory: first

(12) Koch, W.; Frenking, G. *Chem. Phys. Lett.* **1985**, *114*, 178.
(13) Koch, W.; Frenking, G. *J. Chem. Phys.* **1987**, *86*, 5617.
(14) Cooper, D. L.; Wilson, S. *Mol. Phys.* **1981**, *44*, 161.
(15) Fereday, R. J.; Sinha, S. P. *J. Chim. Phys.* **1977**, *74*, 88. We calculated HeOF at all levels employed in this study and found it to be unbound.
(16) Kaufman, J. J.; Sachs, L. M. *J. Chem. Phys.* **1969**, *51*, 2992.
(17) Wilson, S.; Green, S. *J. Chem. Phys.* **1980**, *73*, 419.
(18) Harrison, S. W.; Massa, L. J.; Solomon, P. *Chem. Phys. Lett.* **1972**, *16*, 57.
(19) Wong, M. W.; Nobes, R. H.; Radom, L. *J. Chem. Soc., Chem. Commun.* **1987**, 233.
(20) Schleyer, P. v. R. *Adv. Mass Spectrom.* **1985**, *10a*, 287.
(21) Harrison, S. W.; Henderson, G. A.; Masson, L. J.; Solomon, P. *Astrophys. J.* **1974**, *189*, 605.
(22) (a) Liebman, J. F.; Allen, L. C. *J. Chem. Soc., D* **1969**, 1355. (b) Liebman, J. F.; Allen, L. C. *J. Am. Chem. Soc.* **1970**, *92*, 3539. (c) Liebman, J. F.; Allen, L. C. *Inorg. Chem.* **1972**, *11*, 1143.
(23) (a) Harrison, S. W.; Massa, L. J.; Solomon, P. *J. Chem. Phys.* **1973**, *59*, 263. (b) Hayes, E. F.; Gole, J. L. *J. Chem. Phys.* **1971**, *55*, 5132. (c) Alvarez-Rizzatti, M.; Mason, E. A. *J. Chem. Phys.* **1975**, *63*, 5290.
(24) Hotokka, M.; Kindstedt, T.; Pyykko, P.; Roos, B. O. *Mol. Phys.* **1984**, *52*, 23.
(25) Krauss, M.; Maldonado, P.; Wahl, A. C. *J. Chem. Phys.* **1971**, *54*, 4944.
(26) Catlow, C. W.; McDowell, M. R. C.; Kaufman, J. J.; Sachs, L. M.; Chang, E. S. *J. Phys. B* **1970**, *3*, 833.
(27) Augustin, S. D.; Miller, W. H.; Pearson, P. K.; Schaefer, H. F., III *J. Chem. Phys.* **1973**, *58*, 2845.
(28) (a) Cacace, F. *Adv. Phys. Chem.* **1970**, *8*, 79. (b) Evans, E. A. *Tritium and Its Compounds*; Van Nostrand: London, 1966.
(29) Snell, A. H.; Pleasonton, F. *J. Phys. Chem.* **1958**, *62*, 1377.
(30) Young, S. E.; Coggiola, M. J. *Int. J. Mass Spectrom. Ion Proc.* **1986**, *74*, 137.
(31) Binkley, J. S.; Frisch, M. J.; DeFrees, D. J.; Raghavachari, K.; Whiteside, R. A.; Schlegel, H. B.; Fluder, E. M.; Pople, J. A. GAUSSIAN 82, Carnegie-Mellon University: Pittsburgh, PA.

at the Hartree–Fock (HF) level by using the 6-31G(d,p) basis set[32] and second with inclusion of correlation energy at the Møller–Plesset second-order perturbation level[33] denoted MP2/6-31G(d,p). Vibrational frequencies are calculated in the harmonic approximation to characterize stationary points and to determine zero-point energies (ZPE) at MP2/6-31G(d,p). To account for the errors due to the harmonic approximation, the results are scaled by a factor of 0.93.[34] In some cases the frequencies were obtained at HF/6-31G(d,p) only and subsequently scaled by 0.87.[34] Vibrational frequencies could not be determined by GAUSSIAN82 for higher lying electronic states of a molecule which belong to the same irreducible representation as a lower lying state. In these few cases minima were verified by single-point calculations by using slightly distorted geometries.

By using the optimized geometries, additional single-point energy calculations were made at the full fourth order of Møller–Plesset perturbation theory employing the 6-311G-(2df,2pd) basis set.[35] Thus, the highest level of theory in this study is denoted MP4(SDTQ)/6-311G(2df,2pd)//MP2/6-31G-(d,p) + ZPE. The single-point Møller–Plesset calculations were carried out with the frozen core approximation, while the geometry optimizations used the full core and analytical gradients. Unless otherwise noted, energy values discussed in the paper refer to this level.

For a few molecules, the basis set superposition error (BSSE) has been determined in the calculation of the helium dissociation energy by using the counterpoise method.[36] To this end, the energy of the helium atom was calculated with the complete basis set of the respective molecule in its equilibrium geometry.

For one molecule (HeBeO) calculations have been carried out with the CASSCF (*C*omplete *A*ctive *S*pace SCF) method by using the program GAMESS.[37] The 6-31G(d,p) basis set was employed, and the active space consisted of the full valence and inner-shell space, i.e., orbitals 1–11 (14 electrons in 11 orbitals). For BeO, the active space consisted of 12 electrons in 10 orbitals. The number of configurational state functions was 8674 for HeBeO and 3700 for BeO. The geometries of HeBeO and BeO were optimized by using analytical gradients.[37]

To estimate the bond strengths of the helium bonds in the molecules investigated we calculated the energies of the dissociation reactions yielding He and the respective fragment in the corresponding electronic state to obtain bond dissociation energies (ΔE). Usually, ΔE values are defined as the reaction energies for the homolytic bond cleavage. In the present case, heterolytic bond cleavage was found to be energetically more favorable for most He–X bonds due to the very high ionization energy of He. Thus, we take the bond dissociation energies of the heterolytic fission of the helium bond yielding the fragment in the corresponding electronic state as a measure for the strength of the respective bond.

For some reactions the calculated dissociation energies ΔE have been converted into enthalpies ΔH at T K via eq I[38]

$$\Delta H(T) = \Delta E + \Delta\mathrm{ZPE} + \Delta E_v(T) + \Delta E_r(T) + \Delta E_t(T) + \Delta PV \quad \text{(I)}$$

where ΔZPE is the difference in the zero-point vibrational energies of the reaction partners. $\Delta E_v(T)$, $\Delta E_r(T)$, and $\Delta E_t(T)$ are the corresponding energy differences for the vibrational (v), rotational (r), and translational (t) energy corrections at T K. The molecular contributions to ΔZPE and $\Delta E_v(T)$ are evaluated from the calculated frequencies of the normal modes, while the remaining terms in eq I can be expressed by appropriate multiples of RT.[38]

The analysis of the one-electron density distribution $\rho(\mathbf{r})$ is based on the investigation of its critical (stationary) points $\mathbf{r}_s$, which are the sources and sinks of the gradient paths (trajectories) of the gradient vector field $\nabla\rho(\mathbf{r})$.[39] Of particular interest are the properties of $\rho(\mathbf{r})$ at the critical points $\mathbf{r}_b$ in the internuclear region of two bonded atoms A and B.[40] The value $\rho(\mathbf{r}_b) = \rho_b$ corresponds to the minimum of $\rho(\mathbf{r})$ along a path of maximum electron density (MED path) connecting A and B, i.e., ρ_b is a saddle point of $\rho(\mathbf{r})$ in three dimensions. The MED path can be considered as an image of the bond AB. However, a MED path is also found in the case of closed-shell interactions (e.g., van der Waals interactions, hydrogen bonds, etc.). In order to distinguish between the latter and covalent bonds, the energy density $H(\mathbf{r})$ is used.[41] For all molecules considered to date, $H(\mathbf{r}_b) = H_b$ has turned out to be negative (positive) in case of covalent bonding (closed-shell interactions). Therefore it has been suggested[41,42] that the definition of a covalent bond is based on two conditions, namely (i) the existence of a critical point $\mathbf{r}_b$ and its associated MED path linking the nuclei in question (*necessary condition*) and (ii) $H_b < 0$ which indicates that the accumulation of electron charge in the internuclear region is stabilizing (*sufficient condition*). If condition (ii) is fulfilled, we call the MED path a "bond-path" and $\mathbf{r}_b$ the bond critical point.

The properties of the bond path and bond critical point can be used to characterize the bond, e.g., ρ_b to obtain the bond order n, the position $\mathbf{r}_b$ to determine the bond polarity, the anisotropy ϵ to assess the π-character, or the bend of the MED path to describe the bent bond character.[42,43] Information about bonding can be substantiated by analyzing the Laplacian of $\rho(\mathbf{r})$, $\nabla^2\rho(\mathbf{r})$, which is indicative of concentration ($\nabla^2\rho(\mathbf{r}) < 0$) and depletion ($\nabla^2\rho(\mathbf{r}) > 0$) of electron density.[41,44] The Laplace distribution $\nabla^2\rho(\mathbf{r})$ has been found to reflect the shell structure of atoms.[44] In molecules, concentration lumps can be associated to electron bond pairs and electron lone pairs on the basis of simple models.

By analysis of $\rho(\mathbf{r})$ and its associated Laplace field, the Laplace concentration $\nabla^2\rho(\mathbf{r})$, useful descriptions of bonding have been obtained for hydrocarbons,[40b,45] three-membered ring compounds and π-complexes,[43,46a] Be compounds,[47] and dications.[7]

Because correlation corrected wave functions proved to be necessary to get reasonable energies and geometries for the He compounds considered, we investigated the influence of correlation corrections on the properties of $\rho(\mathbf{r})$.[46b] However, these lead to only very small changes in the bonding region which do not alter the conclusions drawn from HF densities. Therefore, we used HF densities throughout this work at MP2 geometries by using the 6-31G(d,p) basis set.

(32) Hariharan, P. C.; Pople, J. A. *Theor. Chim. Acta* **1973**, *28*, 213.
(33) (a) Møller, C.; Plesset, M. S. *Phys. Rev.* **1934**, *46*, 618. (b) Binkley, J. S.; Pople, J. A. *Intern. J. Quantum Chem.* **1975**, *9S*, 229.
(34) Hout, R. F.; Levi, B. A.; Hehre, W. J. *J. Comput. Chem.* **1982**, *3*, 234.
(35) Krishnan, R.; Binkley, J. S.; Seeger, R.; Pople, J. A. *J. Chem. Phys.* **1980**, *72*, 650.
(36) (a) Boys, S. F.; Bernardi, F. *Mol. Phys.* **1970**, *19*, 553. (b) Clark, T. *A Handbook of Computational Chemistry*; Wiley: New York, 1985; p 289f.
(37) Guest, M. F.; Kendrick, J.; Pope, S. A. GAMESS Documentation, SERC Daresbury Laboratory, Daresbury, Warrington, WA4 4AD, 1983. (b) Dupuis, M.; Spangler, D.; Wendolowski, J. J. NRCC Software Catalog, Vol. 1, Program no. QG01, 1980.
(38) (a) Lewis, G. N.; Randall, M. *Thermodynamics*; Pitzer, K. S., Brewer, L., Eds.; McGraw-Hill: New York, 1961. (b) Pitzer, K. S. *Quantum Chemistry*; Prentice Hall: Englewood Cliffs, 1961.
(39) Bader, R. F. W.; Nguyen-Dang, T. T.; Tal, Y. *Rep. Prog. Phys.* **1981**, *44*, 893.
(40) (a) Bader, R. F. W.; Slee, T. S.; Cremer, D.; Kraka, E. *J. Am. Chem. Soc.* **1983**, *105*, 5061. (b) Cremer, D.; Kraka, E.; Slee, T. S.; Bader, R. F. W.; Lau, C. D. H.; Nguyen-Dang, T. T.; MacDougall, P. J. *J. Am. Chem. Soc.* **1983**, *105*, 5069.
(41) Cremer, D.; Kraka, E. *Angew. Chem.* **1984**, *96*, 612; *Angew. Chem., Int. Ed. Engl.* **1984**, *23*, 627.
(42) (a) Cremer, D.; Kraka, E. *Croat. Chem. Acta* **1985**, *57*, 1265. (b) Cremer, D. In *Modelling of Structure and Properties of Molecules*; Maksic, Z. B., Ed.; Ellis Horwood: Chichester, in press.
(43) (a) Cremer, D.; Kraka, E. *J. Am. Chem. Soc.* **1985**, *107*, 3800, 3811. (b) Cremer, D.; Kraka, E. In *Molecular Structure and Energetics*; Greenberg, A., Liebman, J., Eds.; VCH Publishers: Deerfield, FL, Vol. 7, in press.
(44) (a) Bader, R. F. W.; MacDougall, P. J.; Lau, C. D. H. *J. Am. Chem. Soc.* **1984**, *106*, 1594. (b) Bader, R. F. W.; Essen, H. *J. Chem. Phys.* **1984**, *80*, 1943.
(45) Cremer, D.; Schmidt, T. *J. Org. Chem.* **1985**, *50*, 2684.
(46) (a) Cremer, D.; Gauss, J. *J. Am. Chem. Soc.* **1986**, *108*, 7467. (b) Gauss, J.; Cremer, D., to be published.
(47) Koch, W.; Frenking, G.; Gauss, J.; Cremer, D.; Sawaryn, A.; Schleyer, P. v. R. *J. Am. Chem. Soc.* **1986**, *108*, 5732.

Table I. Calculated Total Energies [hartrees] and Zero-Point Energies ZPE [kcal/mol][d]

molecule		state	symm	HF/6-31G(d,p)// HF/6-31G(d,p)	MP2/6-31G(d,p)// MP2/6-31G(d,p)			E_{tot} for MP2/-, MP3/-, and MP4(SDTQ)/- 6-311G(2df,2pd)//MP2/6-31G(d,p)		
				E_{tot}	E_{tot}	iF	ZPE	MP2/	MP3/	MP4(SDTQ)/
He_2O^{2+}	**1**	$^1A_1$	C_{2v}	−78.8213	−79.0050	0	5.1	−79.0980	−79.1261	−79.1425
He_2N^{2+}	**2**	$^2B_1$	C_{2v}	−58.5919	−58.7246	0	3.6	−58.7826	−58.8101	−58.8224
He_2C^{2+}	**3a**	$^1A_1$	C_{2v}	−42.1352	−42.2422	0	2.0	−42.2797	−42.3066	−42.3174
He_2C^{2+}	**3b**	$^3B_1$	C_{2v}	−42.0807	−42.1630	0	4.9	−42.1995	−42.2154	−42.2203
He_2C^{2+}	**3c**	$^1B_1$	C_{2v}	−41.9909	−42.0903	0	5.3	−42.1304	−42.1539	−42.1637
HeO^+	**4**	$^2\Pi$	$C_{\infty v}$	−77.0281	−77.1517	0[a]	0.8[a]	−77.2283	−77.2501	−77.2587
HeN^+	**5**	$^3\Sigma^-$	$C_{\infty v}$	−56.7259	−56.8143	0	0.4	−56.8357	−56.8738	−56.8797
HeC^{2+}	**6a**	$^1\Sigma^+$	$C_{\infty v}$	−39.2684	−39.3455	0	0.9	−39.3657	−39.3874	−39.3967
HeC^{2+}	**6b**	$^3\Pi$	$C_{\infty v}$	−39.1668	−39.2111	0	2.0	−39.2314	−39.2406	−39.2432
HeC^{2+}	**6c**	$^1\Pi$	$C_{\infty v}$	−39.0595	−39.1250	0[a]	2.1	−39.1481	−39.1679	−39.1783
HeC^+	**7**	$^2\Pi$	$C_{\infty v}$	−40.1430	−40.2161	0	0.2	−40.2352	−40.2547	−40.2615
$HeCCHe^{2+}$	**8a**	$^1\Sigma_g^+$	$D_{\infty v}$	−79.9786	−80.2549	0	9.4	−80.3218	−80.3347	−80.3578
$HeCCHe^{2+}$	**8b**	^3B_u	C_{2h}	−80.0053	−80.2098	0[a]	7.2[a]	−80.2706	−80.3007	−80.3146
$HeCCHe^{2+}$	**8c**	$^3B_2$	C_{2v}	−80.0064	−80.2127	0[a]	6.7[a]	−80.2744	−80.3044	−80.3211
He_2CC^{2+}	**9a**	$^1A_1$	C_{2v}	−79.9655	−80.1892	0	7.0	−80.2502	−80.2864	−80.3048
He_2CC^{2+}	**9b**	$^3B_2$	C_{2v}	−80.0098	−80.2087	0	8.2	−80.2707	−80.2977	−80.3140
$HeCC^{2+}$	**10a**	$^1\Sigma^+$	$C_{\infty v}$	−77.0021	−77.2421			−77.2929	−77.3033	−77.3256
$HeCC^{2+}$	**10b**	$^1\Delta$	$C_{\infty v}$	−77.0880[b,c]						
$HeCC^{2+}$	**10c**	$^1A'(2\pi)$	C_s		−77.3044	0	2.9	−77.3484	−77.3670	−77.4070
$HeCC^{2+}$	**10d**	$^3\Pi(3\pi)$	$C_{\infty v}$	−77.1455	−77.3180	1				
$HeCC^{2+}$	**10e**	$^3A''(1\pi)$	C_s	−77.2048	−77.3358	0	3.3	−77.3750	−77.4013	−77.4130
$HeCC^+$	**11**	$^2\Sigma^+$	$C_{\infty v}$	−77.8728	−78.0775	0	8.2	−78.1339	−78.1525	−78.1700
$HeNNHe^{2+}$	**12**	^1A_g	C_{2h}	−113.1272		0[a]	5.9[a]			
$HeOOHe^{2+}$	**13**	^1A	C_2	−153.9743		0[a]	4.6[a]			
$HeCCH^+$	**14a**	$^1\Sigma^+$	$C_{\infty v}$	−78.5586	−78.8271	1 (0)[a]	10.9[a]			
$HeCCH^+$	**14b**	$^1A'$	C_s		−78.8295	0	12.0	−78.8926	−78.9058	−78.9305
HeBBH	**15**	$^1\Sigma_g^+$	$D_{\infty h}$	54.6418	−54.8559	1				
HeCBH	**16**	$^1\Sigma^+$	$C_{\infty v}$	−65.6703	−65.8997	1				
HeBCH	**17a**	$^1\Sigma^+$	$C_{\infty v}$	−65.7159	−65.9637	1 (0)[a]	10.7[a]			
HeBCH	**17b**	$^1A'$	C_s		−65.9681	0	10.3	−66.0324	−66.0453	−66.0696
HeBN	**18**	$^1\Sigma^+$	$C_{\infty v}$	−81.7513		0[a]	4.5[a]			
HeBeO	**19**	$^1\Sigma^+$	$C_{\infty v}$	−92.2710	−92.5428	0	3.3	−92.6359	−92.6217	−92.6575
C^{2+}		^1S	K_h	−36.3992	−36.4437			−36.4473	−36.4632	−36.4710
C^{2+}		^3P	K_h	−36.2267	−36.2323			−36.2373	−36.2382	−36.2386
C^{2+}		^1P	K_h	−36.0870	−36.1226			−36.1298	−36.1473	−36.1610
C^+		^2P	K_h	−37.2871	−37.3344			−37.3419	−37.3565	−37.3624
He^+		^2S	K_h	−1.9936	−1.9936			−1.9981	−1.9981	−1.9981
He		^1S	K_h	−2.8552	−2.8806			−2.8915	−2.8964	−2.8972
C_2^{2+}		$^1\Sigma_g^+(4\pi)$	$D_{\infty h}$	−74.0169	−74.2193			−74.2549	−74.2632	−74.2850
C_2^{2+}		$^1\Sigma_g^+(0\pi)$	$D_{\infty h}$	−74.3007	−74.4462	0	0.5	−74.4711	−74.5137	−74.5333
C_2^{2+}		$^1\Delta_g$	$D_{\infty h}$	−74.1804	−74.4021					
C_2^{2+}		$^3\Pi_u(1\pi)$	$D_{\infty h}$	−74.3145	−74.4507	0	0.9	−74.4456	−74.4741	−74.5012
C_2^{2+}		$^3\Pi_g(3\pi)$	$D_{\infty h}$	−74.1608	−74.3449			−74.3735	−74.3828	−74.4017
C_2^+		$^2\Sigma_u^+(4\pi)$	$D_{\infty h}$	−74.9135	−75.1535	0	3.0	−75.1906	−75.1848	−75.2185
C_2^+		$^2\Pi_u(3\pi)$	$D_{\infty h}$	−74.9770	−75.2500	0	2.0	−75.2834	−75.2759	−75.3253
C_2H^+		$^1\Sigma^+(4\pi)$	$C_{\infty v}$	−75.6198	−75.8585			−75.9038	−75.9127	−75.9387
C_2H^+		$^1\Delta$	$C_{\infty v}$	−75.7290[b]	−75.9111[b]					
C_2H^+		$^3\Pi(3\pi)$	$C_{\infty v}$	−75.7877	−75.9568	0[a]	8.4[a]			
HCB		$^1\Sigma^+$	$C_{\infty v}$	−62.8359	−63.0550			−63.1050	−63.1124	−63.1336
HCB		$^1A'(2\pi)$	C_s	−62.8619	−63.0869	0	6.7	−63.1325	−63.1254	−63.1696
HCB		$^1A'(0\pi)$	C_s	−62.8642	−63.0274			−63.0757	−63.1042	−63.1160
BeO		$^1\Sigma^+$	$C_{\infty v}$	−89.4091	−89.6547	0	1.9	−89.7361	−89.7155	−89.7529
BN		$^1\Sigma^+$	$C_{\infty v}$	−78.8826						

[a] Calculated at HF/6-31G(d,p). [b] Complex orbitals. [c] Not a minimum (see text). [d] iF denotes the number of imaginary frequencies.

3. Results and Discussion

The calculated total energies E_{tot} and zero-point vibrational energies ZPE for the helium-containing molecules **1–19** and their dissociation products are shown in Table I. The theoretically determined vibrational frequencies for **1–19** are exhibited in Table II. The structural data for the calculated helium compounds are listed in Chart I, together with the results for the respective isoelectronic molecules containing hydrogen instead of helium. The calculated geometries for the dissociation products are shown in Table III.

Because of the low polarizability of helium, dications may be expected as suitable binding partners of He. We start our investigations with rather simple systems, i.e., He_2X^{2+} (X = O, N, C). The isoelectronic hydrogen molecules H_2X are well known and can be used for comparison. The He_2X^{2+} dications are then analyzed in order to develop a strategy for searching other systems which may be capable of binding helium.

3.1. He_2X^{2+} (X = O, N, C). The calculated He–X atomic distances in He_2O^{2+} (**1**), He_2N^{2+} (**2**), He_2C^{2+} ($^1A_1$, **3a**), He_2C^{2+} ($^3B_1$, **3b**), and He_2C^{2+} ($^1B_1$, **3c**) are clearly longer compared to the respective X–H bond lengths in the isoelectronic hydrogen compounds (Chart I). At the MP2/6-31G(d,p) level, the differences in bond length between He–X and X–H increase from 0.187 Å (**1**) to 0.303 Å (**2**) and 0.500 Å (**3a**). This may be explained by the decreasing electronegativity from oxygen to nitrogen and carbon. However, the $^3B_1$ and $^1B_1$ states of He_2C^{2+}, **3b** and **3c**, show a dramatic decrease for the He–C distance by more than 0.4 Å compared to the $^1A_1$ state **3a**, while the respective states of CH_2 show only small changes in the C–H bond length. The He–C bond in **3c** is only 0.072 Å longer compared to CH_2

Table II. Calculated Vibrational Frequencies [cm^{-1}][c]

molecule		state	frequency (symm)
He_2O^{2+}	**1**	$^1A_1$	1392 (b_2), 1288 (a_1), 932 (a_1)
He_2N^{2+}	**2**	$^2B_1$	950 (b_2), 937 (a_1), 623 (a_1)
He_2C^{2+}	**3a**	$^1A_1$	576 (a_1), 521 (b_2), 312 (a_1)
He_2C^{2+}	**3b**	$^3B_1$	1397 (b_2), 1285 (a_1), 745 (a_1)
He_2C^{2+}	**3c**	$^1B_1$	1548 (b_2), 1381 (a_1), 762 (a_1)
HeO^+	**4**[a]	$^2\Pi$	541 (σ)
HeN^+	**5**	$^3\Sigma^-$	250 (σ)
HeC^{2+}	**6a**	$^1\Sigma^+$	609 (σ)
HeC^{2+}	**6b**	$^3\Pi$	1425 (σ)
HeC^{2+}	**6c**	$^1\Pi$	1439 (σ)
HeC^+	**7**	$^2\Pi$	142 (σ)
$HeCCHe^{2+}$	**8a**	$^1\Sigma_g^+$	2370 (σ_g), 1822 (σ_u), 1362 (σ_g), 316 (π_u),[b] 192 (π_g)[b]
$HeCCHe^{2+}$	**8b**[a]	^3B_u	1657 (a_g), 911 (a_g), 854 (b_u), 700 (a_g), 481 (a_u), 406 (b_u)
$HeCCHe^{2+}$	**8c**[a]	$^3B_2$	1660 (a_1), 895 (a_1), 733 (b_2), 638 (b_2), 384 (a_1), 350 (a_2)
He_2CC^{2+}	**9a**	$^1A_1$	1433 (a_1), 1367 (b_2), 947 (a_1), 666 (a_1), 312 (b_2), 203 (b_1)
He_2CC^{2+}	**9b**	$^3B_2$	1746 (a_1), 1201 (a_1), 930 (b_2), 819 (a_1), 576 (b_1), 548 (b_2)
$HeCC^{2+}$	**10c**	$^1A'(2\pi)$	1335 (a′), 583 (a′), 100 (a′)
$HeCC^{2+}$	**10a**	$^3A''(1\pi)$	1066 (a′), 807 (a′), 441 (a′)
$HeCC^+$	**11**	$^2\Sigma^+$	2630 (σ_g), 1589 (σ_g), 751 (π)[b]
$HeNNHe^{2+}$	**12**	^1A_g	1608 (a_g), 707 (a_g), 507 (b_u), 501 (a_g), 479 (a_u), 304 (B_u)
$HeOOHe^{2+}$	**13**	^1A	2579 (a), 201 (a), 201 (b), 103 (a), 99 (b), 9 (a)
$HeCCH^+$	**14a**[a]	$^1\Sigma^+$	3061 (σ), 2171 (σ), 1407 (σ), 806 (π),[b] 180 (π)[b]
$HeCCH^+$	**14b**	$^1A'$	3190 (a′), 2044 (a′), 1396 (a′), 718 (a″), 658 (a′), 382 (a′)
HeBCH	**17a**[a]	$^1\Sigma^+$	3129 (σ), 1800 (σ), 858 (σ), 721 (π_u),[b] 134 (π_g)[b]
HeBCH	**17b**	$^1A'$	3215 (a′), 1627 (a′), 834 (a′), 665 (a″), 497 (a′), 357 (a′)
HeBN	**18**[a]	$^1\Sigma^+$	1903 (σ), 787 (σ), 214 (π)[b]
HeBeO	**19**	$^1\Sigma^+$	1408 (σ), 450 (σ), 218 (π)[b]

[a] Calculated at HF/6-31G(d,p). [b] Degenerate mode. [c] Unless otherwise noted, the results were obtained at MP2/6-31G(d,p).

Table III. Calculated Geometries for Structures of Acceptor Molecules[b]

		C–C, C–B, Be–O		C–H		HCC, HCB	
molecule	state	HF	MP2	HF	MP2	HF	MP2
C_2^{2+}	$^1\Sigma_g^+(4\pi)$	1.143	1.200				
C_2^{2+}	$^1\Sigma_g^+(0\pi)$	1.894	2.116				
C_2^{2+}	$^1\Delta(2\pi)$	1.585	1.472				
C_2^{2+}	$^3\Pi_u(1\pi)$	1.728	1.705				
C_2^{2+}	$^3\Pi_g(3\pi)$	1.258	1.300				
C_2^+	$^2\Sigma_u^+(4\pi)$	1.183	1.223				
C_2^+	$^2\Pi_u(3\pi)$	1.316	1.317				
C_2H^+	$^1\Sigma^+(4\pi)$	1.174	1.221	1.076	1.090	180.0	180.0
C_2H^+	$^1\Delta(2\pi)$	1.352[a]	1.386[a]	1.080[a]	1.087[a]	180.0[a]	180.0[a]
C_2H^+	$^3\Pi(3\pi)$	1.253	1.235	1.075	1.080	180.0	180.0
HCB	$^1\Sigma^+(4\pi)$	1.267	1.306	1.059	1.066	180.0	180.0
HCB	$^1A'(2\pi)$	1.493	1.385	1.069	1.166	164.9	74.2
HCB	$^1A'(O\pi)$	1.555	1.547	1.080	1.083	131.7	139.1
BeO	$^1\Sigma^+(4\pi)$	1.295	1.356				

[a] Complex orbitals. [b] HF and MP2 values are calculated with the 6-31G(d,p) basis set. Bond distances are given in Å, bond angles in deg.

($^1B_1$). Thus, the effect of a different electronic structure can be very strong for the bond length to helium, much stronger compared to hydrogen.

It should be noted that the bond angles for all five helium dications are significantly smaller compared to the isoelectronic hydrogen molecules, but the trend is the same showing the sequence **3a < 2 < 1 < 3b < 3c**.

Unlike methylene, the triplet state is not the ground state of the isoelectronic He_2C^{2+}. The theoretical data in Table I predict the $^1A_1$ singlet state **3a** to be 63.8 kcal/mol lower in energy than the $^3B_1$ triplet state **3b**. This result is not unexpected since it is known that electronegative substituents stabilize the singlet relative to the triplet state of carbenes.[48] In case of He_2C^{2+}, the $^1A_1$ singlet state **3a** profits additionally from less Coulomb repulsion due to the much longer bonds compared to **3b**. This is the reason why multiply charged cations in electronic states with short bonds are often higher in energy than states which have longer bonds, whereas for neutral molecules the opposite is usually found.

The Mulliken overlap population[49] (Chart I) and vibrational frequencies (Table II) indicate that the He–X bonds in **1**, **3b**, and **3c** are moderately strong but rather weak in **2** and especially **3a**. The calculated charge distribution points to substantial positive charge at helium in **1**.

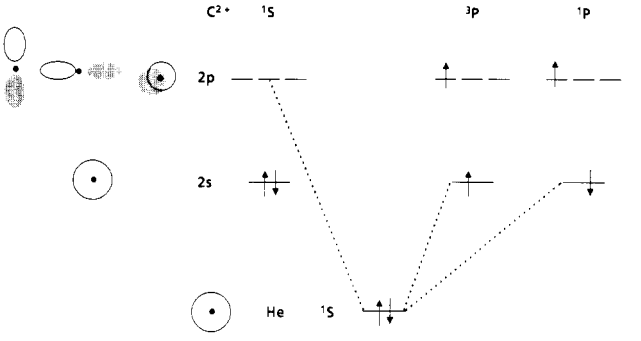

Figure 1. He ^1S interaction with C^{2+} in its ^1S, ^3P, and ^1P states.

What causes the dramatic shortening of the HeC bond distance when going from the $^1A_1$ state of He_2C^{2+} (**3a**) to the $^3B_1$ state

(48) (a) Feller, D.; Borden, W. T.; Davidson, E. R. *Chem. Phys. Lett.* **1980**, *71*, 22. (b) Harrison, J. F.; Liedke, R. C.; Liebman, J. F. *J. Am. Chem. Soc.* **1979**, *101*, 7162.

(49) Mulliken, R. S. *J. Chem. Phys.* **1955**, *23*, 1833.

Chart I. Optimized Geometries of the He Compounds and Isoelectronic H Molecules at MP2/6-31G(d,p)[b]

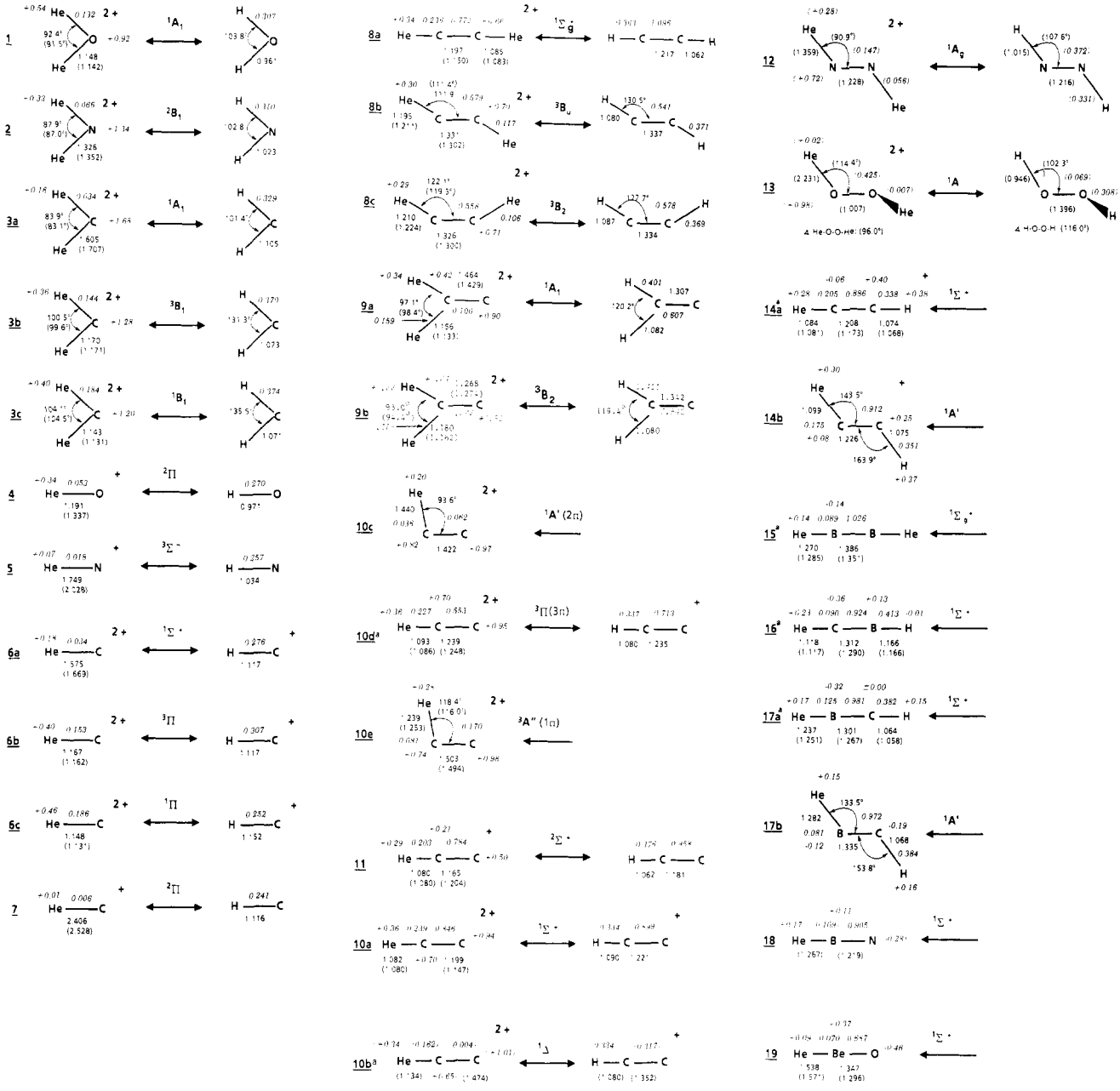

[a] No minimum. [b] HF/6-31G(d,p) results are shown in parentheses. Bond distances are in Å, bond angles in deg. Partial atomic charges for the He compounds and bond population data from the Mullikan population analysis are given in italics.

(**3b**) and $^1B_1$ state (**3c**)? What is the nature of the He–C bond in the different electronic states? We answer these questions in a two-pronged approach, first analyzing the molecular orbitals of the compounds considered and, then, elucidating structural and bonding features by investigating the electron density distribution $\rho(\mathbf{r})$ and its associated Laplacian field $\nabla^2\rho(\mathbf{r})$.

As shown later, most He-containing dications dissociate into neutral helium and a dicationic fragment, rather than He^+ and a monocation. Thus, binding in He dications can be understood as the result of electron donation of the (poor) electron donor He into a dication. Accordingly, He_2C^{2+} dications can be considered to consist of two donor atoms (He) and the acceptor C^{2+} in its ^1S, ^3P, or ^1P state.

The ^3P and ^1P excited states of the carbon dication have a half empty 2s AO, while the lowest unoccupied AO of the ^1S ground state is the 2p orbital. This is schematically shown in Figure 1.

Orbital interaction of ^1S helium with the singly occupied 2s orbital of carbon in its ^3P and ^1P states can be expected to be stronger[50] compared to the higher lying 2p AO in the ^1S state, yielding stronger He–C binding in **3b** and **3c** compared with **3a**. An even stronger interaction should result if both electrons of C^{2+} are excited into p AOs, for example, in its ^1D state.

Figure 2 depicts contour line diagrams of the calculated Laplace distribution $\nabla^2\rho(\mathbf{r})$ of C^{2+}. In its ^1S state C^{2+} possesses a spherical electron distribution $\rho(\mathbf{r})$ as revealed by the Laplacian $\nabla^2\rho(\mathbf{r})$ (Figure 2a). Negative charge shields the carbon nucleus in all directions in space. In the case of the ^3P and ^1P states the electron distribution is anisotropic. As a consequence, the Laplacian concentration of the valence electrons exhibits holes, i.e., locations where negative charge is depleted. This is demonstrated in Figure 2b for the ^3P state of C^{2+}. The carbon nucleus is less shielded in the direction of the holes and, therefore, provides a stronger

(50) This argument is based on the assumption that the interaction of a doubly occupied orbital with a singly occupied MO is stabilizing which is dependent on the size of the overlap of the interacting orbitals: Bernardi, F.; Epiotis, N. D.; Cherry, W.; Schlegel, H. B.; Whangbo, M. H.; Wolfe, S. *J. Am. Chem. Soc.* **1976**, *98*, 469.

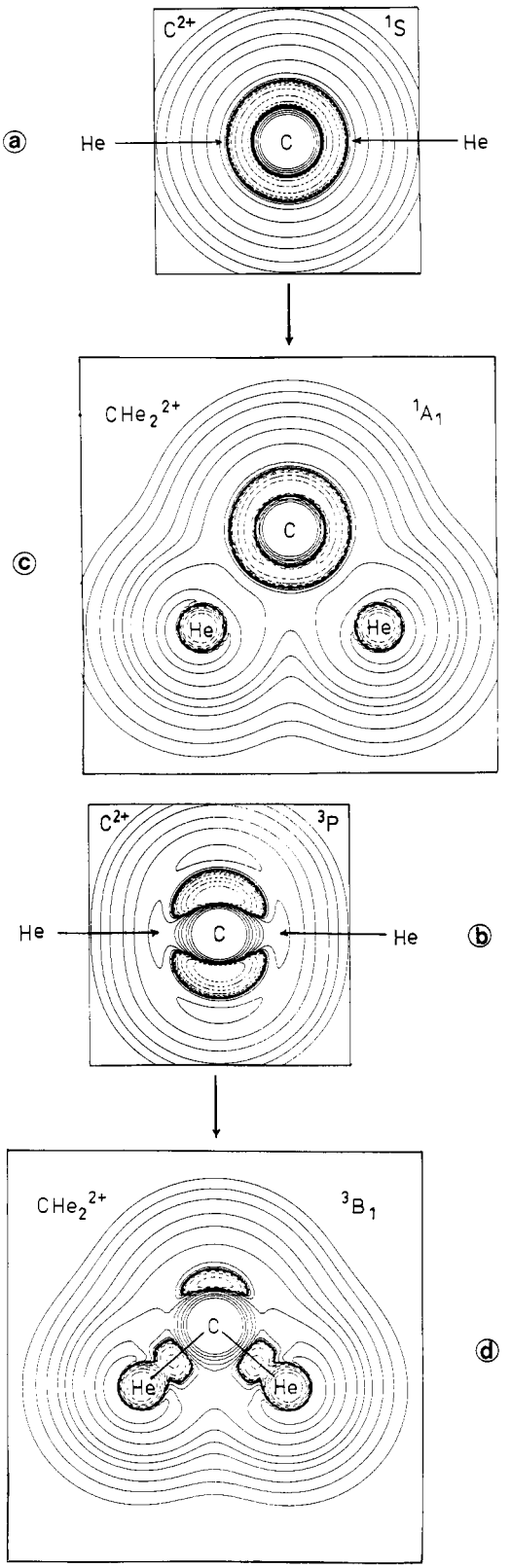

Figure 2. Contour line diagrams of the Laplace concentration $-\nabla^2\rho(\mathbf{r})$ of (a) the ^1S state of C^{2+}, (b) the ^3P state of C^{2+}, (c) the $^1A_1$ state of He_2C^{2+} (**3a**), and (d) the $^3B_1$ state of He_2C^{2+} (**3b**). Dashed contour lines are in regions of charge concentration and solid lines in regions of charge depletion. Inner-shell concentrations are not shown. Heavy solid lines indicate bond paths.

acceptor for the He 1s electrons compared to the ^1S state.

Inspection of the calculated contour line diagrams of the Laplace concentration of He_2C^{2+} in its $^1A_1$ (**3a**) and $^3B_1$ (**3b**) states (Figure 2 (parts c and d)) confirms this prediction, showing striking differences between **3a** and **3b**. **3a** is best described as

Table IV. Characterization of Bonds AB of Acceptor Molecules with the Aid of the Local Properties of Electron and Energy Density (HF/6-31(d,p) Calculations)

molecule	state	R_{AB}	ρ_b	H_b	$n(CC)^b$
CC^{2+}	$^1\Sigma^+_g(0\pi)$	2.116	0.61	−0.2	0.35
CC^{2+}	$^1\Delta_g(2\pi)$	1.472	1.38	−1.2	0.73
CC^{2+}	$^1\Sigma^+_g(4\pi)$	1.200	2.27[a]	−3.3	1.73
CC^{2+}	$^3\Pi_g(3\pi)$	1.300	1.93[a]	−2.4	1.25
CC^+	$^2\Sigma^+_u(4\pi)$	1.223	1.97[a]	−2.7	1.30
CCH^+	$^1\Delta(2\pi)$	1.386	2.27	−2.8	1.73
CCH^+	$^1\Sigma^+(4\pi)$	1.221	2.23[a]	−3.1	1.66
BeO	$^1\Sigma^+$	1.356	1.10	−0.1	

[a] Values indicate cases where a spurious maximum was found that vanishes when larger basis sets are used (compare with acetylene, ref 40a, Table III). The value of ρ at such a maximum exceeds those of neighboring minima by less than 1%. Accordingly, the n values are slightly too large. This can be corrected by averaging ρ over maximum and adjacent minima. [b] The CC bond order has been obtained from $n = \exp[a(\rho_b - b)]$ with $a = 0.96$ and $b = 1.70$ e/Å^3 taken from ref 40a.

Scheme I. Calculated Reaction Energies for He Dissociation of Structures **1–6c** at MP4(SDTQ)/6-311G(2df,2pd)//MP2/6-31G(d,p) + ZPE

He_2O^{2+} (**1**) → $He^+ + HeO^+$ (**4**)	−76.0 kcal/mol	(1)
He_2N^{2+} (**2**) → $He^+ + HeN^+$ (**5**)	−37.9 kcal/mol	(2)
He_2C^{2+} (**3a**) → $He + HeC^{2+}$ (**6a**)	+13.6 kcal/mol	(3a)
He_2C^{2+} (**3a**) → $He^+ + HeC^+$ (**7**)	+34.4 kcal/mol	(3b)
He_2C^{2+} (**3b**) → $He + HeC^{2+}$ (**6b**)	+47.2 kcal/mol	(4a)
He_2C^{2+} (**3b**) → $He^+ + HeC^+$ (**7**)	−29.3 kcal/mol	(4b)
He_2C^{2+} (**3c**) → $He + HeC^{2+}$ (**6c**)	+52.1 kcal/mol	(5a)
He_2C^{2+} (**3c**) → $He + HeC^{2+}$ (**6a**)	−86.0 kcal/mol	(5b)
He_2C^{2+} (**3c**) → $He^+ + HeC^+$ (**7**)	−65.2 kcal/mol	(5c)
HeC^{2+} (**6a**) → $He + C^{2+}(^1S)$	+17.0 kcal/mol	(6a)
HeC^{2+} (**6a**) → $He^+ + C^+(^2P)$	+21.8 kcal/mol	(6b)
HeC^{2+} (**6b**) → $He + C^{2+}(^3P)$	+65.3 kcal/mol	(7a)
HeC^{2+} (**6b**) → $He^+ + C^+(^2P)$	−75.6 kcal/mol	(7b)
HeC^{2+} (**6c**) → $He + C^{2+}(^1P)$	+73.2 kcal/mol	(8a)
HeC^{2+} (**6c**) → $He + C^{2+}(^1S)$	−121.2 kcal/mol	(8b)
HeC^{2+} (**6c**) → $He^+ + C^+(^2P)$	−116.3 kcal/mol	(8c)

the result of closed-shell interaction between C^{2+} and two He atoms with vanishingly small distortions of the spherical Laplace concentrations of the atoms. There are no covalent He–C bonds as revealed by the very low ρ_b and H_b values for the He–C bonds in **3a** (Table V). In contrast to this, the Laplace concentrations of the He atoms in **3b** are strongly distorted in the direction of the C^{2+} acceptor (Figure 2d). The two-dimensional representation of $\nabla^2\rho(\mathbf{r})$ of He has a dropletlike appendage similar to a key that fits into a lock, in this case the hole in the valence sphere of C^{2+}. Such a Laplace concentration is typical for semipolar bonds and, thus, suggests that in **3b** the He atoms are bound to the acceptor C^{2+} by semipolar bonds.

This description is confirmed by the properties of the electron and energy density at $\mathbf{r}_b$(HeC): In **3b** and **3c** ρ_b is more than twice as large as in **3a**. The rather large negative values of $H_b = -1.2$ and −1.3 indicate covalent helium–carbon bonds in **3b** and **3c** (Table V). The bond critical point in **3b** and **3c** is shifted by 26% toward C consistent with the description of a semipolar He–C bond.

The investigation of the electron density reveals that the anisotropy of the charge distribution can be more important than the total charge of the acceptor for binding helium. An anisotropic electron distribution of C^{2+} is caused by exciting one electron from an s orbital to a p orbital, creating an "s-hole". An s electron shields the nucleus uniformly, while a p electron does not. Thus, the creation of an s-hole increases the electron-accepting ability and polarizing power of the acceptor C^{2+}. As a consequence, a short semipolar He–C bond results. The dramatic decrease of

Table V. Characterization of the Bonds in He Compounds with the Aid of the Local Properties of Electron and Energy Density (HF/6-31G(d,p) Calculations)

molecule		bond	R	ρ_b	H_b	∇r_b[c]	n[b]	ΔE[d]	bond character[e]
He_2C^{2+}	**3a**	HeC	1.605	0.49	−0.1	4.3 (He)	0.16	13.6	elec
He_2C^{2+}	**3b**	HeC	1.170	1.16[a]	−1.2	26.5 (C)	0.60	47.2	c, semi
He_2C^{2+}	**3c**	HeC	1.143	1.25[a]	−1.3	26.3 (C)	0.72	52.1	c, semi
$HeCCHe^{2+}$	**8a**	CC	1.197	2.48[a]	−3.6	0.0 (C)	2.12		c
		HeC	1.085	1.38	−1.3	24.6 (C)	0.92	84.7	c, semi
$HeCCHe^{2+}$	**8b**	CC	1.331	2.43	−2.9	0.0 (C)	2.02		c
		HeC	1.195	1.03	−1.2	22.3 (C)	0.46	*f*	c, semi
$HeCCHe^{2+}$	**8c**	CC	1.326	2.36	−2.8	0.0 (C)	1.88		c
		HeC	1.210	1.00	−1.1	21.7 (C)	0.44	*f*	c, semi
He_2CC^{2+}	**9a**	CC	1.464	1.85	−2.0	12.6 (C)	1.15		c
		HeC	1.156	1.09[a]	−1.0	26.2 (C)	0.52	51.4	c, semi
He_2CC^{2+}	**9b**	CC	1.268	2.43	−4.1	31.8 (C)	2.02		c
		HeC	1.180	1.07[a]	−1.1	25.1 (C)	0.50	*f*	c, semi
$HeCC^{2+}$	**10a**	CC	1.199	2.35[a]	−3.4	1.2 (C)	1.87		c
		HeC	1.082	1.42	−1.4	24.5 (C)	1.00	89.9	c, semi
$HeCC^{2+}$	**10c**	CC	1.422	1.61	−1.6	4.1 (C)	0.95		c
		HeC	1.409	0.70	−0.5	9.2 (C)	0.24	*f*	elec
$HeCC^{2+}$	**10e**	CC	1.503	1.83	−1.7	3.1 (C)	1.13		c
		HeC	1.234	0.94	−1.0	23.0 (C)	0.39	71.5	c, semi
$HeCC^{+}$	**11**	CC	1.165	2.74[a]	−4.3	2.9 (CHe)	2.72		c
		HeC	1.080	1.27	−1.0	24.3 (C)	0.74	28.8	c, semi
$HeCCH^{+}$	**14b**	CC	1.226	2.56	−4.4	27.5 (CHe)	2.29		c
		HeC	1.099	1.17	−0.9	24.9 (C)	0.61	23.7	c, semi
HeBeO	**19**	BeO	1.347	1.15	−0.2	29.4 (Be)			elec
		HeBe	1.538	0.17	0.1	17.2 (Be)		3.0	elec

[a] See fnt *a*, Table IV. [b] See fnt *b*, Table IV. The bond orders n for the HeC bond have been determined from $n = \exp[1.97(\rho_b - 1.42)]$. Reference bonds are the HeC bonds of $HeCC^{2+}$ (**10a**) and He_2C^{2+} ($^1A_1$), the n values of which have been set to 1.00 and 0.16, respectively, according to the calculated dissociation energies of 89.9 and 13.6 kcal/mol. [c] Shift of the bond critical point r_b relative to the midpoint of the bond in direction of the less electronegative atom given in parentheses. [d] Dissociation energies have been taken from Schemes I, II, III, and IV. [e] c and semi denote covalent, semipolar bonds; elec indicates a closed-shell interaction, e.g., ionic bonding or electrostatic attraction due to dipole, induced dipole or induced dipole, induced dipole interactions. [f] Could not be determined, see text.

the HeC distance when going from the $^1A_1$ ground state to the $^3B_1$ or $^1B_1$ excited state of He_2C^{2+} is due to the s-hole in the electronic structure of the respective states of C^{2+}.

What are the stabilities of **1–3** toward dissociation? Scheme I shows the calculated energies of reaction for the dissociation of **1–3** (reactions 1–5). The energetically most favorable dissociation reactions for **1** and **2** are the charge-separation reactions 1 and 2, since the second ionization energies for oxygen and nitrogen are much higher than the first ionization energy of helium.[5] Both reactions are clearly exoenergetic. For singlet He_2C^{2+}, the dissociation to neutral helium is energetically more favorable. Scheme I shows that $He^+ + HeC^+$ is a higher energy pathway for the singlet states **3a** and **3c** compared to $He + HeC^{2+}$. For the triplet state **3b** the charge separation reaction 4b leading to He^+ and HeC^+ is more favorable compared to reaction 4a since the $^3\Pi$ state of HeC^{2+} (**6b**) is too high in energy to make reaction 4a compatible.

The calculated dissociation energies for helium dissociation from **3a**, **3b**, and **3c** to HeC^{2+} in the corresponding electronic states can be used to estimate the ΔE values of the helium–carbon bonds (reactions 3a, 4a, and 5a). The ΔE for **3a** is only +13.6 kcal/mol (reaction 3a), but for **3b** and **3c** the values are +47.2 and +52.1 kcal/mol, respectively (reactions 4a and 5a). Thus, the He–C bond in the $^1A_1$ ground state of He_2C^{2+} is clearly weaker compared to the excited $^3B_1$ and $^1B_1$ states.

The energetic stabilities for the ground states of He_2X^{2+} toward dissociation are predicted to increase with decreasing electronegativity of X, i.e., **1** < **2** < **3a**, and the $^1A_1$ ground state of He_2C^{2+} is calculated to be stable relative to all possible dissociation products. In order to substantiate this result further, we converted the calculated energy of reaction 3a into the corresponding reaction enthalpy. Under laboratory conditions, T is set to 298 K. Then, the translational and rotational corrections and ΔPV of eq I for reaction 3a lead to $+2RT = +1.2$ kcal/mol. The vibrational correction at T is −0.5 kcal/mol when the calculated harmonic frequencies are used to estimate $\Delta E_v(T)$.[38] Thus, the theoretically predicted enthalpy of reaction 3a at 298 K is +14.3 kcal/mol.

What is the reliability of this result, and what changes can be expected if higher levels of theory are employed? A theoretical investigation of the atomization energies of AH_n molecules including H_2O, H_2N, and H_2C, which are isoelectronic to structures **1–3**, revealed that with the theoretical level employed in our study the deviation from experimentally derived values is less than 5 kcal/mol.[52] Our calculated results for the bond lengths in **3a** (Chart I) show rather large changes for different levels of theory. Doubly charged species are more difficult to compute than neutral compounds.[11] However, any improvement in the theoretical treatment of reactions 1–5 should therefore lower the energy of the reactants; i.e., species **1–3** should benefit more than the dissociation products. This means that our computed energies shown in Scheme I should be considered as lower bounds, and we predict that He_2C^{2+} in its $^1A_1$ ground state is a thermodynamically stable molecule.

Whether the other dications **1**, **2**, **3b**, and **3c** are observable as metastable species will depend on the barrier for the reactions 1, 2, 4, and 5. Work is in progress to determine the dissociation barriers at the MCSCF level of theory.[53]

The sequence in He–C bond lengths and bond dissociation energies calculated for He_2C^{2+} **3a**, **3b**, and **3c** is also found for the primary dissociation product HeC^{2+} in the corresponding electronic states, i.e., **6a**, **6b**, and **6c** (Table I and Chart I). The $^1\Sigma^+$ ground state **6a** has a comparatively long atomic distance (1.575 Å), which is much shorter in the excited $^3\Pi$ state **6b** (1.167 Å) and $^1\Pi$ state **6c** (1.148 Å). The corresponding states of isoelectronic CH^+ have nearly the same C–H distances (Chart I). The bond dissociation energies for **6a**, **6b**, and **6c** are more positive (reactions 6–8, Scheme I) but show the same trend compared with **3a–3c**. HeC^{2+} (**6a**) is stable toward helium dissociation with a bond dissociation energy of +17.0 kcal/mol (reaction 6a). Triplet **6b** has a bond dissociation energy of +65.3 kcal/mol (reaction 7a), but the charge separation reaction 7b is strongly exoenergetic by −75.6 kcal/mol. The shortest bond and highest bond disso-

(51) Duley, W. W.; Williams, D. A. *Interstellar Chemistry*; Academic Press: London, 1984.
(52) Pople, J. A.; Frisch, M. J.; Luke, B. T.; Binkley, J. S. *Int. J. Quantum Chem.: Quant. Chem. Symp.* **1983**, *17*, 307.
(53) Koch, W.; Frenking, G., to be published.

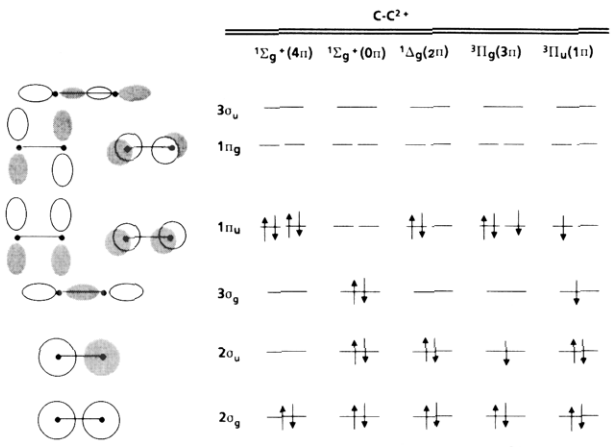

Figure 3. Orbital diagrams for five different states of CC^{2+}. Only one component of the $^1\Delta_g$ state is shown (see ref 60b).

ciation energy (+73.2 kcal/mol, reaction 8a) is found for **6c**, but reaction 8b, which leads to the ^1S ground state of C^{2+}, and the deprotonation reaction 8c are strongly exoenergetic by −121.2 and −116.3 kcal/mol, respectively.

3.2. HeCCHe^{2+} and Related Structures. The investigation of dications He_2X^{2+} discussed in the previous section has shown that an acceptor dication must provide low-lying, empty σ orbitals to bind helium strongly. In terms of the electron density analysis this means that σ holes in the valence shell concentration of an electron acceptor are necessary for the formation of covalent, semipolar bonds between helium and the acceptor. The question is whether the creation of σ holes by excitation of σ electrons to π orbitals requires more or less energy than gained by the formation of the helium–acceptor bond. Molecules with triple bonds contain a relatively high (low) number of $\pi(\sigma)$ electrons and are suitable candidates to examine this question. To this end we investigated diheliumacetylene dication HeCCHe^{2+} **8a**.

The optimized geometry of HeCCHe^{2+} **8a** is shown in Chart I, together with the calculated data for isoelectronic acetylene. The He–C bond length in **8a** is even shorter compared with **3b** and **3c**. The calculated value of 1.085 Å is in the range of a typical C–H atomic distance and only slightly longer compared to the C–H bond in acetylene. The theoretically predicted He–C stretching frequency is 2370 cm^{-1} (Table II) while for acetylene the experimentally derived value[54] is 3373 cm^{-1}. Both data indicate fairly strong helium–carbon bonding. Helium carries about half the positive charge of what is found for the carbon atoms in **8a**.

The structure of HeCCHe^{2+} (**8a**) can be rationalized by considering **8a** as donor–acceptor complex of CC^{2+} in its corresponding electronic state ($^1\Sigma^+_g$ with 4 π electrons) and two helium atoms. The $^1\Sigma^+_g(4\pi)$ state of CC^{2+} is schematically shown in Figure 3, together with several other electronic states.[55] The $^1\Sigma^+_g(4\pi)$ state has a very low-lying empty $2\sigma_u$ orbital which explains the strong electron-acceptor ability yielding a short He–C bond with a bond length of 1.085 Å. In contrast, the ground state of CC^{2+} ($^1\Sigma^+_g(0\pi)$, Figure 3)[55] has no π electrons, but the $2\sigma_u$ and $3\sigma_g$ MOs are occupied. We were unable to locate a minimum structure containing a He–C bond which correlates to the $^1\Sigma^+_g(0\pi)$ state of CC^{2+}.

The above argument is based on idealized molecular orbitals without allowing for hybridization. The actual occupied valence orbitals of HeCCHe^{2+} (**8a**), using STO-3G wave functions, are shown in Figure 4, together with the corresponding MOs of acetylene. The $2\sigma_g$ and $2\sigma_u$ orbitals of HeCCHe^{2+} (**8a**) consist of the symmetric and antisymmetric combinations of the He 1s AOs with carbon sp hybrids, and the two lowest lying valence MOs of **8a** are dominantly He–C bonding. The $3\sigma_g$ MO of **8a** is mainly C–C bonding. This is in contrast to acetylene where the $2\sigma_g$ MO is dominantly C–C bonding and the $2\sigma_u$ and $3\sigma_g$ MOs are C–H bonding. The orbital plots for **8a** demonstrate that large He 1s coefficients are found only in the two lowest lying σ MOs, with only small He 1s participation in the $3\sigma_g$ orbital.

The donor–acceptor model explains the effect of replacing the carbon atoms in HeCCHe^{2+} (**8a**) by nitrogen and oxygen yielding HeNNHe^{2+} (**12**) and HeOOHe^{2+} (**13**). We calculated **12** and **13** at the HF/6-31G(d,p) level. For the isoelectronic hydrogen compounds HNNH and HOOH, shorter bond lengths to hydrogen are found with increasing electronegativity C < N < O (Chart I). For the He-containing dications **8a**, **12**, and **13** the results are opposite, much longer atomic distances are reported for the helium bonds with nitrogen and oxygen (Chart I). NN^{2+} and OO^{2+} have two and four more electrons, respectively, compared to CC^{2+}. Orbital interaction of the $^1\Sigma^+_g(4\pi)$ states with helium is only possible via the $3\sigma_g$ LUMO (NN^{2+}) or $1\pi_g$ LUMO (OO^{2+}) which are higher lying than the $2\sigma_u$ MO (Figure 3). The result shows clearly that less electronegative elements with a lower number of valence electrons bind helium better than more electronegative elements with a higher number of electrons.

More striking are the results of the electron density analysis. In Figure 5 contour line diagrams and perspective drawings of $\nabla^2\rho(\mathbf{r})$ are shown for the $^1\Sigma^+_g$ states of CC^{2+} with 0π electrons (Figure 5 (parts a and b)) and with 4π electrons (Figure 5 (parts c and d)). The differences are obvious. The latter state exhibits large areas of electron depletion (holes) in the direction of the nuclear axis, resembling the shape of the $2\sigma_u$ LUMO (Figure 3). These σ holes are absent for the $^1\Sigma^+_g(0\pi)$ state, which shows smaller holes in the direction of the pπ LUMO (Figure 5b). The perspective drawings indicate that concentrations of the (total) valence electrons are particularly high at positions where the HOMO of the molecule possesses its largest amplitude. Thus, the distribution $\nabla^2\rho(\mathbf{r})$ reflects the nature of the frontier orbitals.

Besides HeCCHe^{2+} (**8a**), two more helium dications have theoretically been found which correlate to $CC^{2+}(4\pi)$. Electron donation by one helium atom leads to HeCC^{2+} (**10a**), which is also calculated with a short (1.082 Å, Chart I) He–C bond. Electron donation at the terminal carbon atom by a second helium atom leads to HeCCHe^{2+} (**8a**). If both helium atoms are bound to the same carbon atom, the vinylidene structure **9a** will be formed. The He–C bonds in **9a** are slightly longer (1.156 Å) compared with **8a** and **10a**, and the overlap population and frequency data indicate weaker He–C bonds in **9a**. The calculated energies (Table I) predict that the linear isomer **8a** is only 28.4 kcal/mol lower in energy than **9a**, while the calculated vinylidene/acetylene energy difference is 46 kcal/mol.[56]

The shapes of the Laplace fields $\nabla^2\rho(\mathbf{r})$ for **8a**, **9a**, and **10a** shown in Figure 6 reveal further details concerning the He–C bond. The charge concentration at the helium atom is significantly deformed, similar to the deformation found for **3b**. The results shown in Table V indicate that the He–C bond in **8a** and **10a** is somewhat stronger compared with **3b**. The CC bond becomes stronger by successive helium binding, as is indicated by ρ_b, H_b, and n, listed in Tables IV and V. Electronic charge donated by He contributes to the screening of the carbon nuclei, thus lowering nuclear–nuclear repulsion.

Are there other electronic states of CC^{2+} besides $^1\Sigma^+_g(4\pi)$ which are capable of attracting helium to form a He–C bond? As noted before, the $^1\Sigma^+_g(0\pi)$ ground state (Figure 3) does not form a He-containing molecule. Another possible candidate is the $^1\Delta_g$ state schematically shown in Figure 3. The lowest lying empty orbital is the $3\sigma_g$ MO, and weaker He–C bonding relative to the He compounds related to the $^1\Sigma^+_g(4\pi)$ state (**8a**, **9a**, **10a**) is predicted. Our calculations revealed that HeCC^{2+} in the corresponding linear $^1\Delta$ state **10b** is not a minimun on the potential energy hypersurface. **10b** is subject to Renner distortion,[57] and

(54) Herzberg, G. *Molecular Spectra and Molecular Structure II. Infrared and Raman Spectra of Polyatomic Molecules*; Van Nostrand: New York, 1945; p 180.

(55) Besides the five different states for C_2^{2+} listed in Table I, we calculated the following states: $^1\Sigma^-_g(2\pi)$, $^1\Pi_u(3\pi)$, $^1\Pi_u(1\pi)$, $^1\Pi_g(3\pi)$, $^3\Pi_u(3\pi)$, $^3\Pi_g(3\pi)$, $^3\Sigma^-_g(2\pi)$, and $^5\Sigma^-_u(2\pi)$. None of these states was lower in energy than the $^1\Sigma^+_g(0\pi)$ state.

(56) At the MP4(SDTQ)/6-311G(d,p)//MP2/6-31G(d) level, acetylene is predicted to be 45.9 kcal/mol lower in energy than vinylidene.[59]

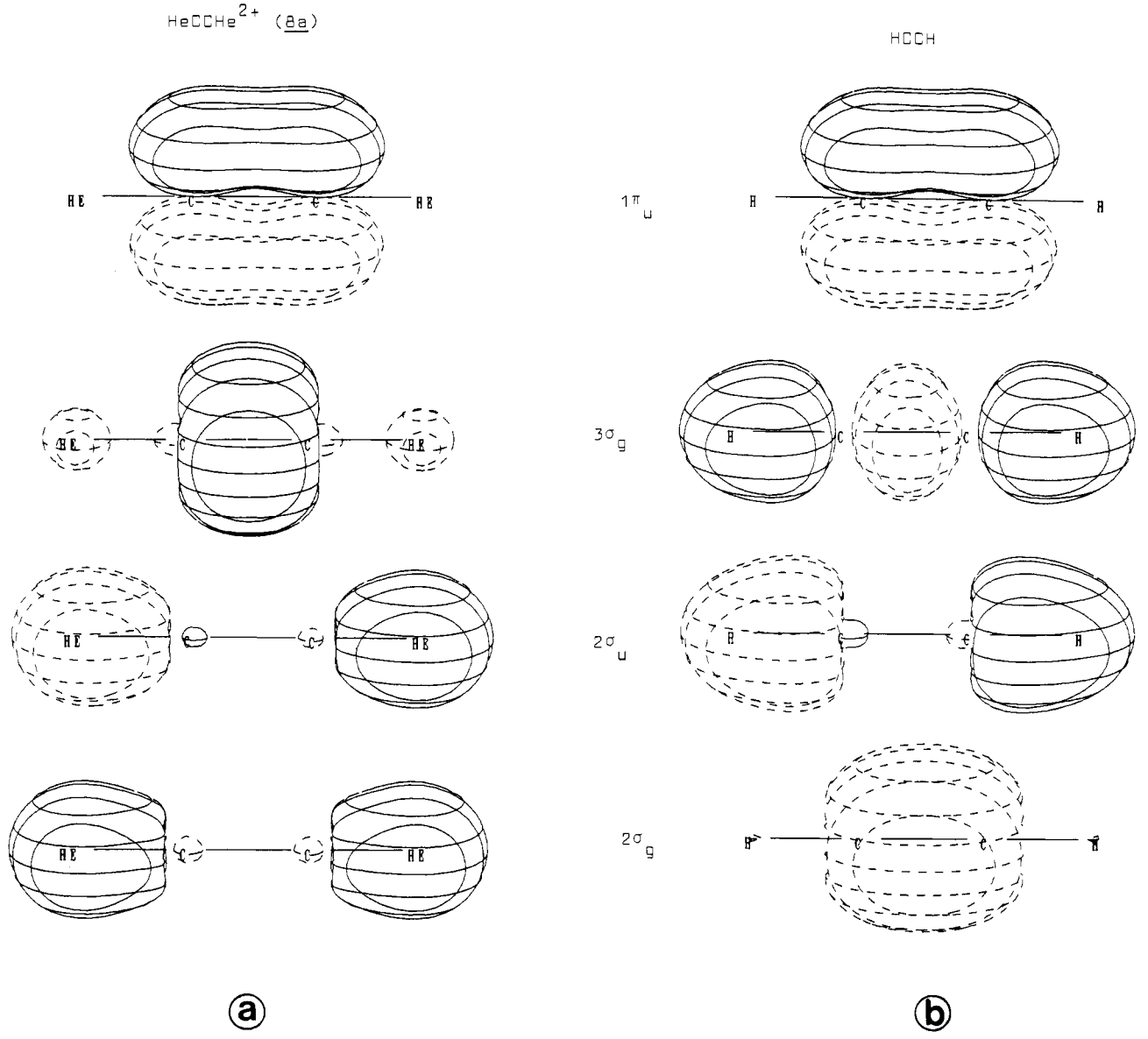

Figure 4. Orbital plots of the occupied valence orbitals of (a) $HeCCHe^{2+}$ **8a** and (b) acetylene, using STO-3G wave functions at MP2/6-31G(d,p) optimized geometries.

bending of **10b** leads to two different $^1A'$ states, one with two and the other with zero π electrons. The mixing of the orbitals upon bending of the $^1\Delta$ state is shown in Figure 7 with use of Walsh-type diagrams.[58] When the orbitals are filled with the six electrons of the CC^{2+} acceptor, it is obvious that the 5a′ LUMO of the $^1A'(2\pi)$ state is lower in energy than the 1a″ LUMO of the $^1A'(0\pi)$ state (Figure 7). Consequently, the former state forms a He–C bond (structure **10c**), but the latter does not. The strongly bent structure **10c** exhibits a much longer (1.440 Å) He–C bond compared with **10a**. Furthermore, **10c** is not capable of attracting a second helium atom; no minimum could be located for $He_2C_2^{2+}$ related to the $^1\Delta_g$ state of CC^{2+}. However, **10c** is lower in energy than **10a** by 51.0 kcal/mol (Table I). This is a further example that isomeric structures of dications with weaker (longer) bonds may be lower in energy than isomers with stronger (shorter) bonds since the Coulomb repulsion is higher in the latter.

Upon approach of a helium atom, the *concentric* Laplace concentration of the $^1\Delta_g$ state of CC^{2+} changes to the one shown in Figure 8 (parts a and b) which can be considered as a (noninteracting) $^1A'$ complex of He and CC^{2+} with two π electrons in a MO perpendicular to the plane of the complex. The π holes in the plane of the approaching helium atom are clearly visible in the contour line diagram, while the carbon atoms in the perpendicular plane are much more shielded due to the two π-electrons. The shape of the Laplacian distribution makes it plausible that the resulting helium dication has a nonlinear geometry. Figure 8c exhibits the contour line diagram of structure **10c**. Unlike structures **8a** or **10a** (Figure 6), He is hardly polarized by CC^{2+} in **10c**. There is no indication of a semipolar bond between donor and acceptor, in sharp contrast to what is found for **10a** (Figure 6a). On the other hand, the carbon nuclei are much more shielded in **10c** which explains why this state is lower in energy than **10a**. The analysis of $\rho(\mathbf{r})$ (Table V) shows that He–C interaction is significantly weaker in **10c** compared with the structure **10a**. According to H_b there is a very weak He–C bond in **10c** which is classified as electrostatic.

Besides the two singlet states, we found a triplet state of CC^{2+}, the $^3\Pi_g(3\pi)$ state (Figure 3) which is capable of forming a He–C bond. The schematic representation in Figure 3 shows that the $^3\Pi_g(3\pi)$ state has a singly occupied $2\sigma_u$ MO. Thus, the He–C bonding capability can be expected to be intermediate between the $^1\Sigma^+_g(4\pi)$ and $^1\Delta_g$ states.[50] Indeed, this was found computa-

(57) (a) Renner, R. *Z. Physik* **1934**, *92*, 172. (b) Herzberg, G.; Teller, E. *Z. Phys. Chem.* **1933**, *B21*, 410.

(58) (a) Walsh, A. D. *J. Chem. Soc.* **1953**, 2260, 2266, 2288, 2296, 2301, 2306, 2318, 2321, 2325, 2330. (b) Gimarc, B. M. *Molecular Structure and Bonding: The Qualitative Molecular Orbital Approach*; Academic Press: New York, 1979.

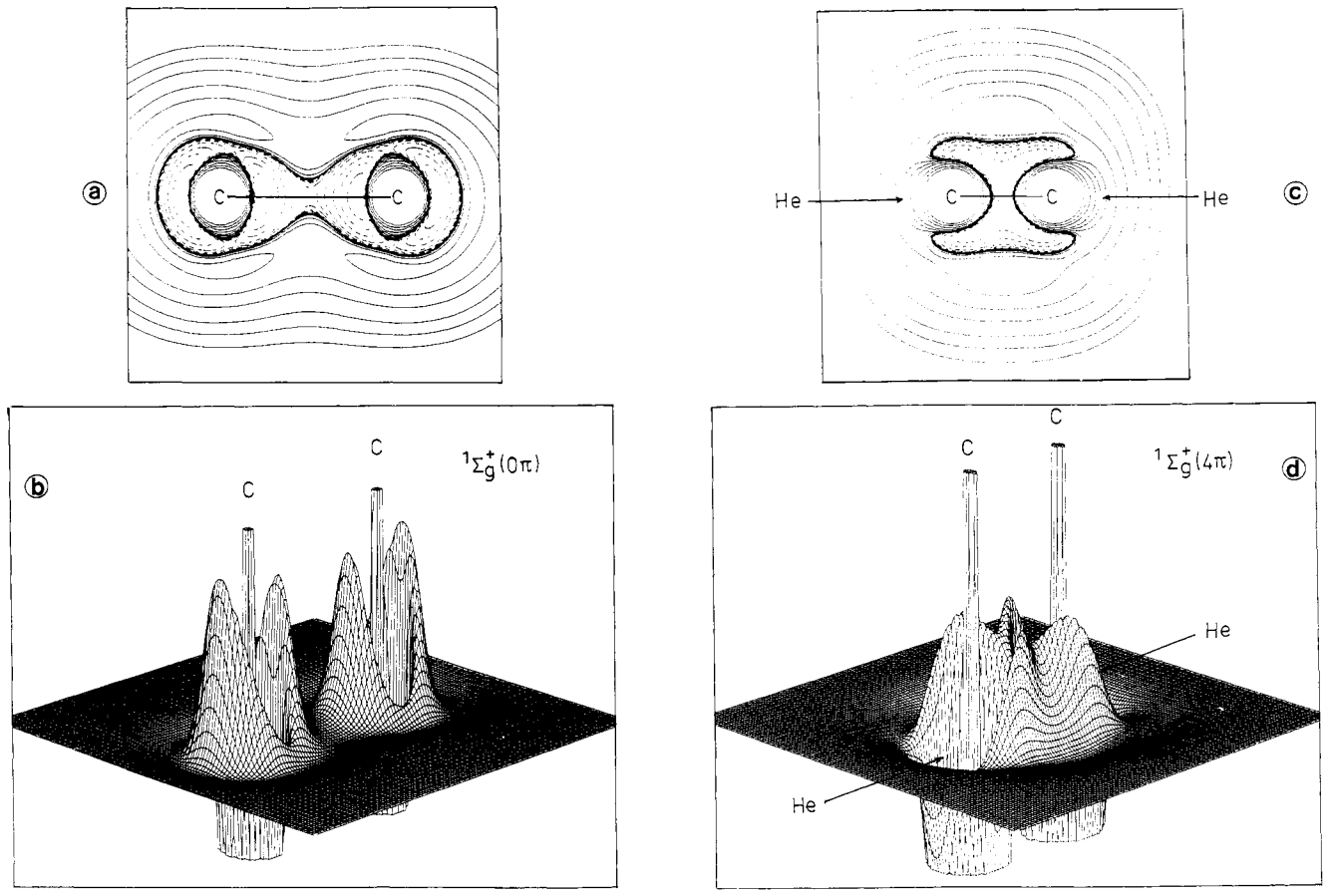

Figure 5. Contour line diagrams and perspective drawings of the Laplace concentration $-\nabla^2\rho(\mathbf{r})$ of the $^1\Sigma^+_g(0\pi)$ state (a and b) and $^1\Sigma^+_g(4\pi)$ state (c and d) of CC^{2+}. Holes are indicated in the contour line diagrams by arrows. See also caption of Figure 2.

tionally. Like the $^1\Delta$ state of $HeCC^{2+}$ (**10b**), the resulting linear $^3\Pi$ state of $HeCC^{2+}$ (**10d**) is also subject to Renner distortion.[57] Figure 7 shows the Walsh-type diagram for orbital mixing upon bending of the $^3\Pi$ state of $HeCC^{2+}$. The $^3A'(2\pi)$ state can be expected to be a better helium (electron) acceptor than the $^3A''(1\pi)$ state.[50] The theoretical result shows that the $^3A'(2\pi)$ state of $HeCC^{2+}$ leads to a linear geometry. Bending toward the $^3A''(1\pi)$ state leads to a nonlinear minimum **10e** with a He–C atomic distance of 1.239 Å (Chart I), intermediate between the values found for **10a** and **10c**. The triplet structure **10e** is predicted to be the energetically lowest lying bound state of $HeCC^{2+}$.

The Renner splitting found for the $^1\Delta$ and $^3\Pi$ states of $HeCC^{2+}$ at the MP2/6-31G(d,p) level is schematically shown in Figure 9. The $^1A'(2\pi)$ and $^3A''(1\pi)$ states exhibit nonlinear minima. The $^1A'(0\pi)$ state leads to helium dissociation while the $^3A'(2\pi)$ state leads to a linear geometry which was calculated to have one negative eigenvalue of the Hessian matrix.

The electron-accepting ability of the $^3\Pi_g$ state of CC^{2+} was found to be strong enough to bind two helium atoms. Two triplet structures were optimized for $HeCCHe^{2+}$, the trans form **8b** and the cis form **8c**. Furthermore, a vinylidene analogue He_2CC^{2+} (**9b**) was found as a ($^3B_2$) triplet. The He–C bond distances are longer in the triplets compared to the respective singlet structures **8a** and **9a** (Chart I). Singlet $HeCCHe^{2+}$ (**8a**) is still lower in energy by 28.3 kcal/mol relative to **8b** and by 26.5 kcal/mol relative to **8c** (Table I). This is much smaller than the isoelectronic hydrogen compounds where the triplet trans (cis) HCCH structure is calculated to be 99.7 (90.8) kcal/mol higher in energy compared to singlet acetylene (MP2/6-31G(d,p)//6-31G(d)).[59] For the vinylidene analogues, triplet **9b** is more stable than singlet **9a** by 4.6 kcal/mol (Table I), whereas triplet H_2CC is predicted to be 46.4 kcal/mol higher in energy than singlet vinylidene (MP2/6-31G(d,p)//6-31G(d)).[59] However, singlet **8a** is still lower in energy than triplet **9b** by 26.3 kcal/mol (Table I). Thus, the singlet diheliumacetylene dication **8a** is the energetically lowest lying bound state on the potential energy hypersurface of $He_2C_2^{2+}$.

The energetically lowest lying triplet state of CC^{2+} was theoretically found to be the $^3\Pi_u(1\pi)$ state which is schematically shown in Figure 3. No minimum could be located for a $HeCC^{2+}$

Scheme II. Calculated Reaction Energies for He Dissociation of Structures **8a–10e** at MP4(SDTQ)/6-311G(2df,2pd)//MP2/6-31G(d,p) + ZPE

$HeCCHe^{2+}$ (**8a**) → He + $HeCC^{2+}$ (**10a**)	+84.7 kcal/mol[a]	(9a)
$HeCCHe^{2+}$ (**8a**) → He + $HeCC^{2+}$ (**10c**)	+27.1 kcal/mol	(9b)
$HeCCHe^{2+}$ (**8a**) → He^+ + $HeCC^+$ (**11**)	+117.8 kcal/mol	(9c)
$HeCCHe^{2+}$ (**8a**) → 2HeC^+ (**7**)	−112.6 kcal/mol	(9d)
$HeCCHe^{2+}$ (**8b**) → He + $HeCC^{2+}$ (**10e**)	−0.6 kcal/mol	(10a)
$HeCCHe^{2+}$ (**8b**) → He^+ + $HeCC^+$ (**11**)	+93.4 kcal/mol	(10b)
$HeCCHe^{2+}$ (**8b**) → 2HeC^+ (**7**)	−137.5 kcal/mol	(10c)
$HeCCHe^{2+}$ (**8c**) → He + $HeCC^{2+}$ (**10e**)	+3.5 kcal/mol	(11a)
$HeCCHe^{2+}$ (**8c**) → He^+ + $HeCC^+$ (**11**)	+97.5 kcal/mol	(11b)
$HeCCHe^{2+}$ (**8c**) → 2HeC^+ (**7**)	−133.4 kcal/mol	(11c)
He_2CC^{2+} (**9a**) → He + $HeCC^{2+}$ (**10a**)	+51.4 kcal/mol[a]	(12a)
He_2CC^{2+} (**9a**) → He + $HeCC^{2+}$ (**10c**)	−3.7 kcal/mol	(12b)
He_2CC^{2+} (**9a**) → He^+ + $HeCC^+$ (**11**)	+86.9 kcal/mol	(12c)
He_2CC^{2+} (**9b**) → He + $HeCC^{2+}$ (**10e**)	−2.5 kcal/mol[a]	(13a)
He_2CC^{2+} (**9b**) → He^+ + $HeCC^+$ (**11**)	+102.5 kcal/mol	(13b)
$HeCC^{2+}$ (**10a**) → He + $CC^{2+}(^1\Sigma^+_g,4\pi)$	+89.9 kcal/mol[a]	(14a)
$HeCC^{2+}$ (**10a**) → He + $CC^{2+}(^1\Sigma^+_g,0\pi)$	−65.8 kcal/mol[a]	(14b)
$HeCC^{2+}$ (**10c**) → He + $CC^{2+}(^1\Sigma^+_g,0\pi)$	−17.1 kcal/mol	(15)
$HeCC^{2+}$ (**10e**) → He + $CC^{2+}(^3\Pi_g,3\pi)$	+71.5 kcal/mol[a]	(16a)
$HeCC^{2+}$ (**10e**) → He + $CC^{2+}(^3\Pi_u,1\pi)$	+6.8 kcal/mol	(16b)

[a] Without ZPE.

(59) *The Carnegie-Mellon Quantum Chemistry Archive*, 3rd ed.; Whiteside, R. A., Frisch, M. J., Pople, J. A., Eds.; Carnegie-Mellon University: Pittsburgh, 1983.

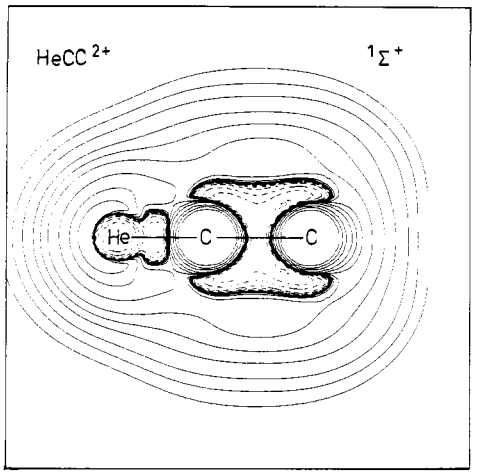

ⓐ

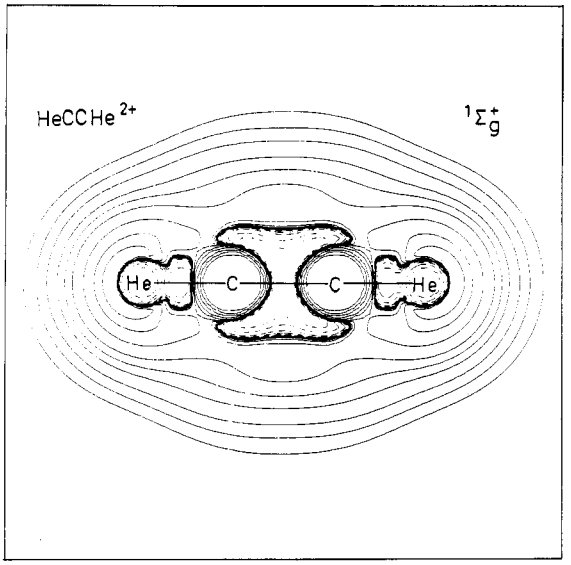

ⓑ

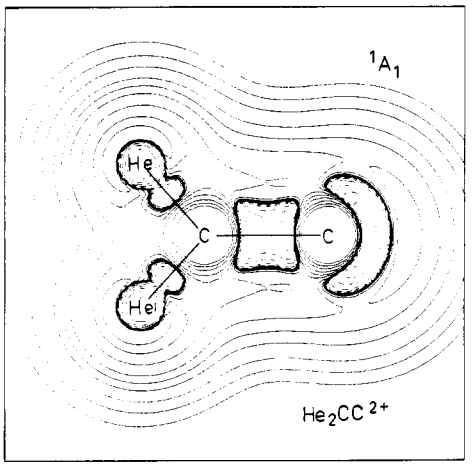

ⓒ

Figure 6. Contour line diagrams of the Laplace concentration $-\nabla^2\rho(\mathbf{r})$ of (a) the $^1\Sigma^+(4\pi)$ state of $HeCC^{2+}$ (**10a**), (b) $HeCCHe^{2+}$ $^1\Sigma^+g(4\pi)$ (**8a**), and (c) He_2CC^{2+} $^1A_1$ (**9a**). See also caption of Figure 2.

dication which is correlated to this electronic state.

The Laplacian distribution $\nabla^2\rho(\mathbf{r})$ of the $^3\Pi_g(3\pi)$ state of CC^{2+} in the two orthogonal planes containing the molecular axis is shown in Figure 10. Two holes are indicated in the direction of the nuclear axis. Here, the preferred deformation toward a nonlinear

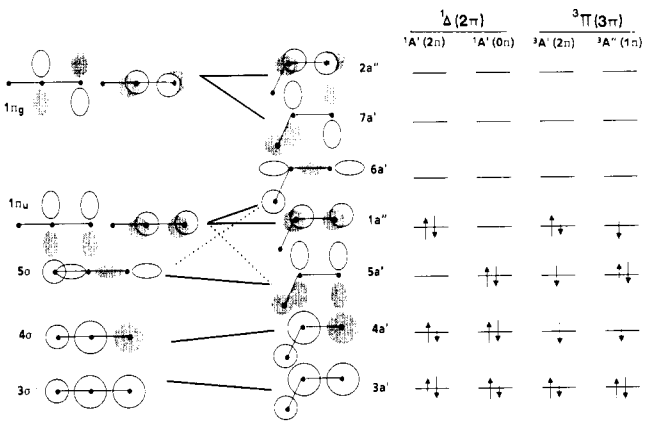

Figure 7. Walsh-type diagrams of the orbital levels for the splitting of the $^1\Delta$ and $^3\Pi$ state of $HeCC^{2+}$. Dotted lines indicate and avoided crossing. The shown electron occupancy arises from the CC^{2+} fragment in the respective electronic state (see text).

arrangement is not immediately obvious. Figure 11 exhibits the contour line diagrams $\nabla^2\rho(\mathbf{r})$ for the triplet helium dications **8b**, **8c**, and **10b**. The He electron density distribution is clearly deformed in these triplet structures indicating semipolar covalent He–C bonding. The calculated data in Table V show that the He–C bond order decreases from 0.92 for **8a** to 0.46 (**8b**) and 0.44 (**8c**); for $HeCC^{2+}$ (**10e**) a value of 0.39 is calculated.

What are the stabilities of structures **8–10** toward dissociation? The calculated reaction energies for the dissociation reactions of ions **8–10** are exhibited in Scheme II. Dissociation of neutral helium from **8a** yielding **10a** (reaction 9a) is energetically favored compared to the charge-separation reaction 9c yielding He^+ and $HeCC^+$ (**11**). Both reactions are strongly endoenergetic, and the data for reaction 9a predict that the bond dissociation energy for the He–C bond in **8a** is +84.7 kcal/mol. This rather high value demonstrates that the helium–carbon bond can be very strong. A substantially lower bond dissociation energy of +51.4 kcal/mol is predicted for He_2CC^{2+} (**9a**) (reaction 12a). This value is comparable in magnitude to what is calculated for He_2C^{2+} in its $^1B_1$ state (**3c**) (+52.1 kcal/mol reaction 5a, Scheme I). If the dissociation of $HeCCHe^{2+}$ (**8a**) yields $HeCC^{2+}$ in its $^1A'$ state (**10c**) (reaction 9b) the reaction is still endoenergetic by +27.1 kcal/mol, while for He_2CC^{2+} (**9a**) the corresponding reaction 12b is now slightly exoenergetic by −3.7 kcal/mol.

In contrast to the fission of the He–C bond, breaking the C–C bond in **8a** is a very exoenergetic process by −112.6 kcal/mol (reaction 9d). However, a substantial activation barrier for this reaction can be expected although the bond order derived from the electron density analysis (Table V) and also the Mulliken overlap population (Chart I) indicates that the C–C bond in **8a** is weaker compared to acetylene. Our results predict that **8a** is a metastable dication which, once it has been produced, should have a sufficient lifetime to be detected in the gas phase.

For the triplet states **8b**, **8c**, and **9b** the bond strength could not be determined from the calculation of bond dissociation energies because the corresponding triplet state of $HeCC^{2+}$ (**10d**) is not a minimum on the potential energy surface. Helium dissociation leads in all cases to $HeCC^{2+}$ (**10e**), and the reactions are predicted to be energetically nearly balanced (reactions 10a, 11a, and 13a). As for **8a**, dissociation of He^+ from **8b**, **8c**, and **9b** is much more unfavorable (reactions 10b, 11b, and 13b) compared to the dissociation of neutral He.

The calculated value for the dissociation energy of $^1\Sigma^+$ $HeCC^{2+}$ (**10a**) to helium and C_2^{2+} ($^1\Sigma^+_g(4\pi)$) indicates that the bond dissociation energy for the helium–carbon bond in **10a** is +89.9 kcal/mol (reaction 14a), comparable to what is found for **8a** (reaction 9a). Dissociation of **10a** into He and the ground state of C_2^{2+} ($^1\Sigma^+_g(0\pi)$) is exoenergetic by −65.8 kcal/mol (reaction 14b). We are presently investigating the dissociation reactions of structures **8–11** at the MCSCF level.[53]

The He–C distances in **10c** and **10e** are clearly longer compared to **10a**, and this should be reflected in lower bond dissociation

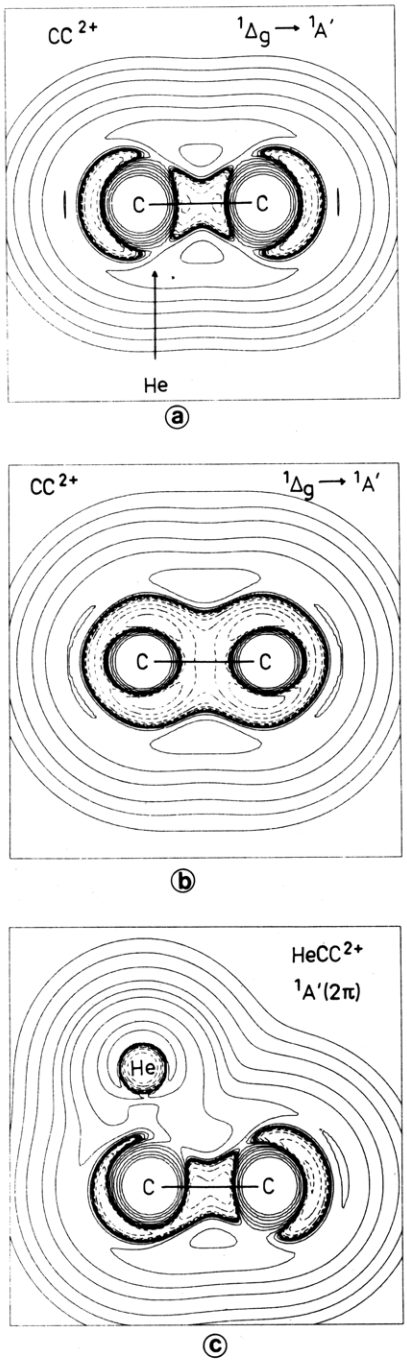

Figure 8. Contour line diagrams of the Laplace concentration $-\nabla^2\rho(\mathbf{r})$ of the $^1\Delta_g$ state of CC^{2+} in the xz plane (a) and yz plane (b) upon approach of an He atom in the xz plane; MO π_x is empty, and MO π_y is doubly occupied. Note that due to the presence of an He atom the symmetry of the $^1\Delta_g$ state is broken, and, therefore, the description with real orbitals leading to a $^1A'$ state is justified. (c) Laplace concentration of $HeCC^{2+}$ (**10c**) in the molecular plane. See also caption of Figure 2.

energies. The electronic state of CC^{2+} corresponding to **10c** is the $^1\Delta_g$ state. We were not able to calculate this state by using complex orbitals and thus do not attempt to estimate the bond dissociation energy of **10c** leading to CC^{2+} ($^1\Delta_g$).[60] Helium dissociation from **10c** yielding the $^1\Sigma^+_g(0\pi)$ ground state of CC^{2+} is predicted to be exoenergetic by −17.1 kcal/mol (reaction 15). The corresponding triplet state of CC^{2+} for **10e** is the $^3\Pi_g(3\pi)$ state, and the bond dissociation energy of **10e** is calculated as +69.2 kcal/mol (reaction 16a). Dissociation of **10e** into the $^3\Pi_u(1\pi)$ state of CC^{2+}, which was calculated as the lowest lying triplet state, is still endoenergetic by +6.8 kcal/mol (reaction 16b).

(60) (a) The geometries, but not the energies, of Δ states can be sometimes mimicked by (not correctly) using real rather than complex orbitals within the single-determinant approach. For example, the total energy of CCH^+ optimized with the 6-31G(d,p) basis set using complex orbitals is 12.7 kcal/mol lower than with real orbitals, but the geometries are nearly identical: C–C 1.356 Å (real), 1.352 Å (complex), C–H 1.079 Å (real and complex).[59] (b) For a discussion of Δ states and the use of real and complex orbitals to describe them see: Salem, L. *Electrons in Chemical Reactions*; Wiley: New York, 1982; p 67f.

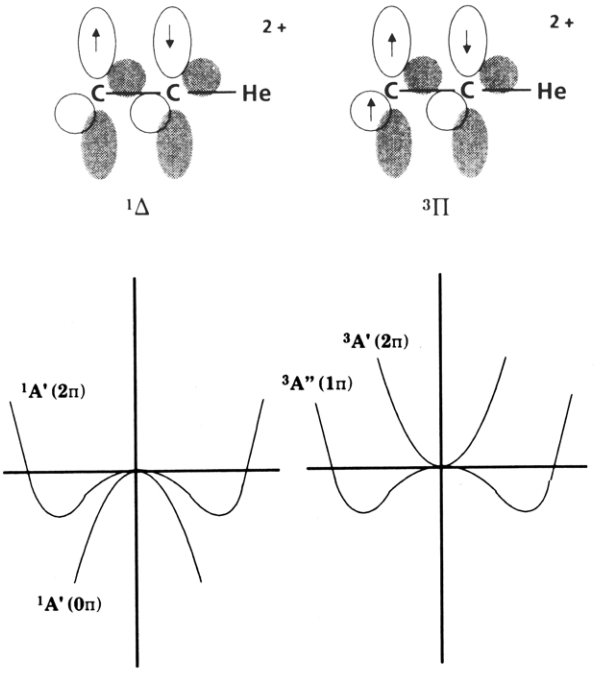

Figure 9. Schematic representation of the Renner splitting for the $^1\Delta$ and $^3\Pi$ states of $HeCC^{2+}$. Only one component of the $^1\Delta$ state is shown (see ref 60b).

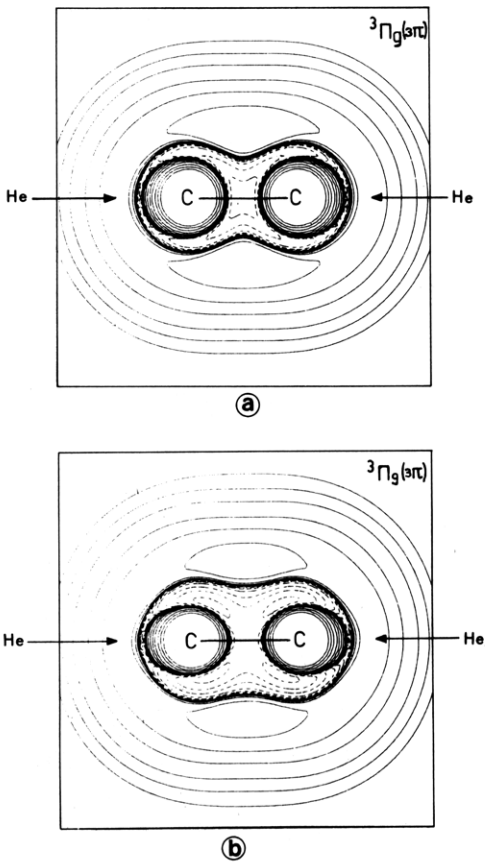

Figure 10. Contour line diagrams of the Laplace concentration $-\nabla^2\rho(\mathbf{r})$ of the $^3\Pi_g(3\pi)$ state of CC^{2+} in the xz plane (a) and yz plane (b). MO π_x is singly occupied, and MO π_y is doubly occupied. See also caption of Figure 2.

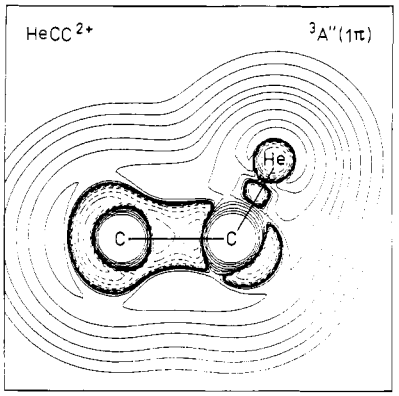

ⓐ

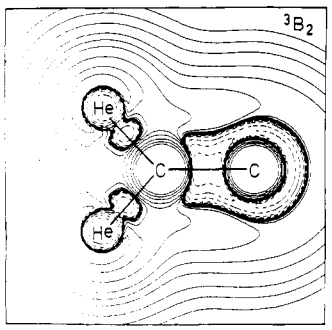

ⓑ

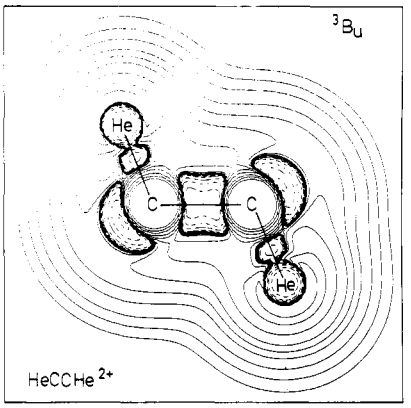

ⓒ

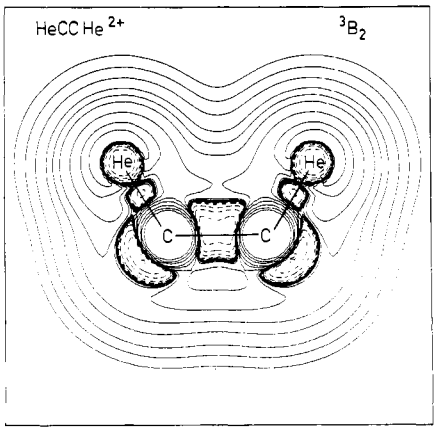

ⓓ

Figure 11. Contour line diagrams of the Laplace concentration $-\nabla^2\rho(\mathbf{r})$ of structures **10e** (a), **9b** (b), **8b** (c), and **8c** (d). See also caption of Figure 2.

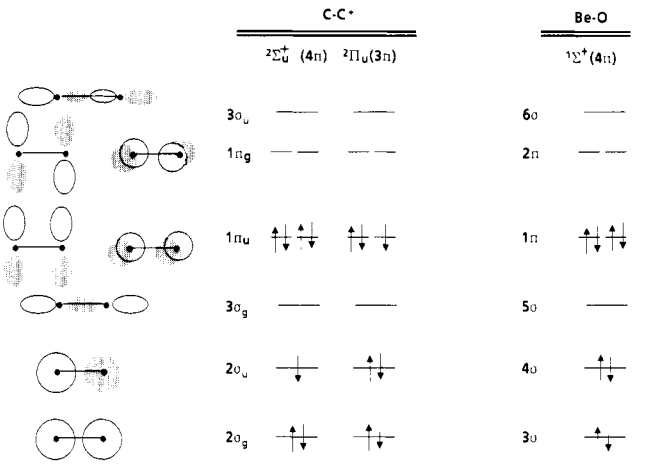

Figure 12. Orbital diagrams for two different electronic states of CC^+ and the ground state of BeO.

Scheme III. Calculated Reaction Energies for He Dissociation of Structures **11** and **14b** at MP4(SDTQ)/6-311G(2df,2pd)//MP2/6-31G(d,p) + ZPE

$HeCC^+$ (**11**) → He + $CC^+(^2\Sigma^+_u,4\pi)$	+28.8 kcal/mol	(17a)
$HeCC^+$ (**11**) → He + $CC^+(^2\Pi_u,1\pi)$	−39.1 kcal/mol	(17b)
$HeCCH^+$ (**14b**) → He + $CCH^+(^1\Sigma^+)$	+59.3 kcal/mol[a]	(18a)
$HeCCH^+$ (**14b**) → He + $CCH^+(^1\Delta)$	+23.7 kcal/mol[b]	(18b)

[a] Without ZPE. [b] At MP2/6-31G(d,p) using complex orbitals for CCH^+.

3.3. $HeCC^+$ and $HeCCH^+$. The theoretically obtained results discussed so far stress the decisive role of the electronic structure of an acceptor atom or molecule in regard to its ability to bind helium in a chemical bond. Depending on the electronic state CC^{2+} may (i) bind He strongly as in **8a** or **10a**, (ii) form a weaker, but still covalent He–C bond as in **8b**, **8c**, or **10e**, (iii) lead to a very weak bond classified as electrostatic as in **10c**, or (iv) not lead to a He–C bond at all as is the case for the $^1\Sigma^+_g(0\pi)$ ground state[55] of CC^{2+}. The analysis of the electron density of electron acceptor species and the resulting He compounds has shown that the presence of valence concentration "holes", especially those with σ symmetry, is crucial for establishing a chemical bond with helium. Perhaps this is even more important than the Coulomb attraction of the highly charged dication. This result prompted us to search for *mono*cations which might be able to form a helium bond. We investigated $HeCC^+$ (**11**) and $HeCCH^+$ (**14**).

The donor–acceptor model outlined above suggests that the $^2\Sigma^+_u(4\pi)$ state of CC^+ should provide a suitable electronic structure for binding helium. A schematic representation of the $^2\Sigma^+_u(4\pi)$ state of CC^+ is shown in Figure 12, together with the $^2\Pi_u(3\pi)$ state which was found to be the lowest lying doublet state of CC^+.[61] The $2\sigma_u$ orbital is singly occupied in the $^2\Sigma^+_u(4\pi)$ state. The Laplacian distribution of this state is shown in Figure 13 and should be compared with the $^1\Sigma^+_g(4\pi)$ state of CC^{2+} shown in Figure 5 (parts c and d). In both cases, two σ holes are found, but it is obvious that the σ holes are larger in the dication compared with the monocation where the holes are more easily visible in the three-dimensional diagram shown in Figure 13b.

The corresponding He cation $HeCC^+$ (**11**, $^2\Sigma^+(4\pi)$) is calculated to have a short (1.080 Å) He–C bond (Chart I). The $\nabla^2\rho(\mathbf{r})$ plot of **11** shown in Figure 13c indicates that the Laplace distribution at He is clearly deformed as a result of the bond formation. The calculated data for the bond order n and energy density H_b (Table V) support the classification of the He–C bond in **11** as covalent and semipolar. The Laplace distribution in Figure 13c suggests that $HeCC^+$ (**11**) will not bind another helium

(61) Besides the two states of C_2^+ listed in Table I, we calculated the $^2\Delta_g(2\pi)$, the $^4\Sigma^+_u(2\pi)$, and $^4\Pi_g$ states. The $^4\Sigma^-_g$ state was found to be the ground state and the $^2\Pi_u$ state the lowest lying doublet state, which is in agreement with earlier theoretical investigations: Petrongolo, C.; Bruna, P. J.; Peyerimhoff, S. D.; Buenker, R. J. *J. Chem. Phys.* **1981**, *74*, 4594.

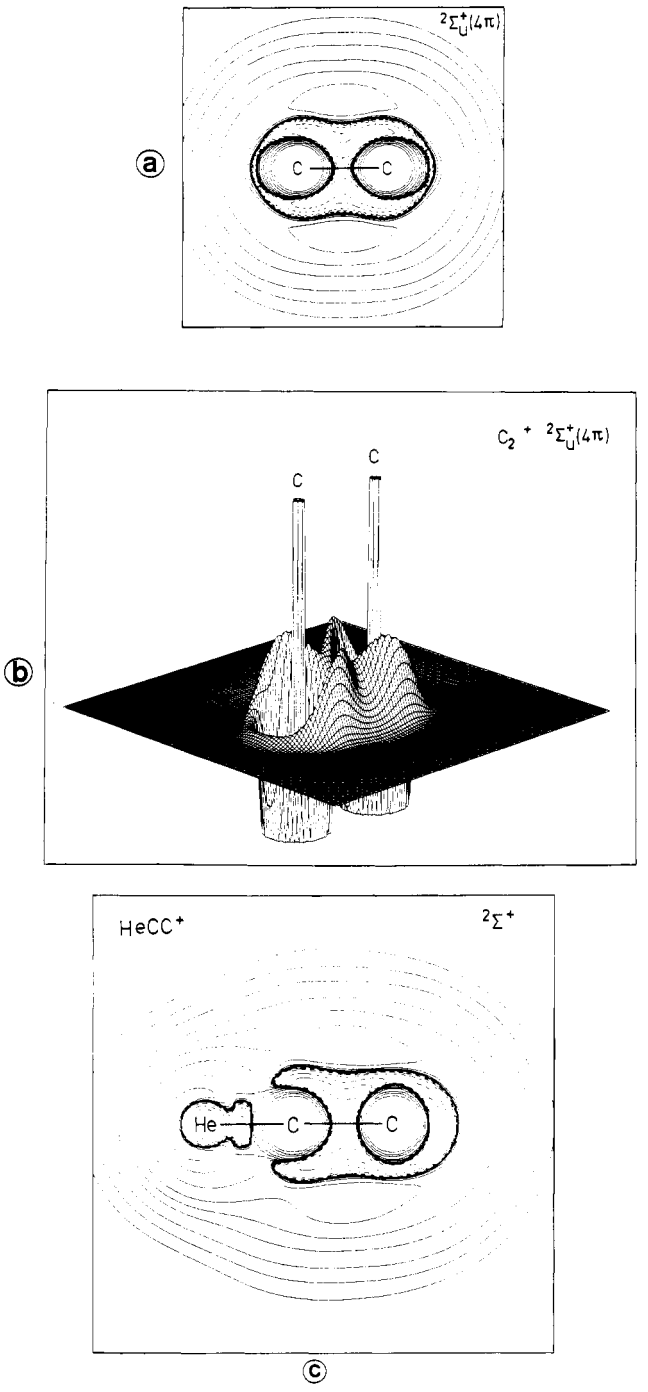

Figure 13. (a) Perspective drawing and (b) contour line diagram of the Laplace concentration $-\nabla^2\rho(\mathbf{r})$ of the $^2\Sigma^+_g(4\pi)$ state of CC^+; (c) contour line diagram of the Laplace concentration $-\nabla^2\rho(\mathbf{r})$ of $HeCC^+$ **11**. See also caption of Figure 2.

atom since there is no longer a σ hole in the valence concentration of the terminal C atom. In fact, $HeCCHe^+$ was not found to be a bound molecule.

Like dication **10a**, the monocation $HeCC^+$ (**11**) is stable toward helium loss if the corresponding $^2\Sigma^+_u$ state of CC^+ is formed. The bond dissociation energy of the He–C bond in **11** is much lower (+28.8 kcal/mol, reaction 17a, Scheme III) compared to the dications **8a** and **10a**. Dissociation into the lowest lying doublet $^2\Pi_u$ state[61] of C_2^+ is exoenergetic by −39.1 kcal/mol (reaction 17b).

Structure **11** was the only bound state of $HeCC^+$ which could be located as a minimum on the potential energy hypersurface. Thus, the $^2\Sigma^+_u(4\pi)$ state of CC^+ (Figure 12) is the only low-lying electronic state which forms a He–C bond. Other electronic states of $HeCC^+$ besides **11** were theoretically found to be unbound. Again, this is in sharp contrast to the isoelectronic hydrogen compounds. CCH has a $^2\Sigma^+$ ground state.[62] However, the first excited $^2\Pi$ state of CCH has nearly the same C–H bond lengths as the ground state.[62]

Since the monocation $HeCC^+$ (**11**) was found with a short He–C bond and a still substantially positive bond dissociation energy of +28.8 kcal/mol, we investigated $HeCCH^+$ (**14**). $HeCCH^+$ has already been studied theoretically by Cooper and Wilson,[14] and a linear geometry with a He–C bond length of 1.24 Å, clearly longer compared with $HeCCHe^{2+}$ (**8a**), was reported. Our results for **14** are quite different.[63] Optimization of **14** at the 6-31G(d,p) level yielded a linear structure **14a** with bond distances very similar to $HeCCHe^{2+}$ (Chart I). The He–C bond length at this level is calculated as 1.081 Å. However, at the MP2/6-31G(d,p) level the linear structure is no longer a minimum. Rather, a trans bent geometry **14b** was located with a slightly longer (1.099 Å) He–C bond. A corresponding cis structure was not found. The energy difference between the minimum structure **14b** and the linear form **14a** at the MP2/6-31G(d,p) level is rather small (1.5 kcal/mol, Table I).

Initially, the nonlinear geometry of $HeCCH^+$ (**14b**) is surprising. $HeCCH^+$ is isoelectronic with acetylene, and, thus, a linear geometry might be expected. The donor–acceptor model provides an explanation for the unexpected geometry. $HeCCH^+$ can be considered as the product of He and CCH^+. CCH^+ has a triplet ground state,[64] but for the present discussion only singlet states are of interest. Like isoelectronic $HeCC^{2+}$ (**10**), CCH^+ has low-lying $^1\Sigma^+(4\pi)$ and $^1\Delta$ singlet states (compare **10a** and **10b**). Unlike $HeCC^{2+}$ (**10b**), the $^1\Delta$ state of CCH^+ is a minimum on the potential energy hypersurface.[64] At the MP2/6-31G(d,p) level of theory using complex orbitals, the $^1\Delta$ state of CCH^+ is 33.0 kcal/mol lower in energy than the $^1\Sigma^+$ state (Table I).

The Laplacian distribution of the two singlet states of CCH^+ is shown in Figure 14. The $^1\Sigma^+(4\pi)$ state exhibits a large σ hole in the direction of the nuclear axis, while the $^1\Delta$ state shows only rather small π holes. Unlike the $^1\Sigma^+_g(4\pi)$ and $^1\Delta_g$ states of CC^{2+}, which lead to two different $HeCC^{2+}$ structures **10a** and **10c** (compare Figures 6a and 8c), only one bound state **14b** emerges for $HeCCH^+$. The Laplace concentration is shown in Figure 14. It is obvious that the electronic structure of $HeCCH^+$ (**14b**) results from electron donation of He into a mixture of the $^1\Sigma^+(4\pi)$ and $^1\Delta$ states of CCH^+. The Laplace distribution at He is clearly deformed, and the data for the bond order n and H_b (Table V) indicate that the He–C bond in **14b** is covalent, semipolar, and slightly weaker compared with $HeCC^+$ (**11**).

An important result shown in Scheme III is the predicted stability of $HeCCH^+$ toward dissociation of He yielding CCH^+ in a singlet state. Taking the ΔE of reaction 18b, the dissociation energy of the He–C bond in **14b** is 23.7 kcal/mol, 5.1 kcal/mol lower than the value found for $HeCC^+$ (**11**) (reaction 17a).[66]

3.4. Neutral Helium Compounds. The result that helium is rather strongly bound even in a monocation such as $HeCCH^+$ and that the electronic structure of an acceptor atom or molecule is more important than the positive charge for attracting electronic charge from helium suggests the intriguing possibility that helium may form a chemical bond to a suitable electron acceptor in the ground state of a *neutral* molecule. Our findings suggest HeBBHe (**15**), HeCBH (**16**), and HeBCH (**17**) as possible candidates.

(62) (a) Shih, S.; Peyerimhoff, S. D.; Buenker, R. J. *J. Mol. Spectrosc.* **1977**, *64*, 167; **1979**, *74*, 124. (b) Goebel, J. H.; Bregman, J. D.; Cooper, D. M.; Goorvitch, D.; Langhoff, S. R.; Witteborn, F. C. *Astrophys. J.* **1983**, *270*, 190.

(63) The results in ref 14 have been obtained by using a minimum (STO-3G) basis set. We found that at least a split-valence (3-21G) basis set has to be employed for molecules with short bonds to helium such as **8a**, **10a**, and **11** to yield consistent data for the He–X atomic distances. Further extension of the theoretical level up to MP2/6-31G(d,p) changes the 3-21G optimized He–C bond length very little.

(64) Krishnan, R.; Frisch, M. J.; Whiteside, R. A.; Pople, J. A.; Schleyer, P. v. R. *J. Chem. Phys.* **1981**, *74*, 4213.

(65) Δ states with complex orbitals could only be calculated at MP2/6-31G(d,p) as the highest level of theory.

(66) If the ΔE of reactions 17a and 18b are compared at the same (MP2/6-31G(d,p)//MP2/6-31G(d,p)) level of theory (Table I), the difference is reduced to 3.5 kcal/mol.

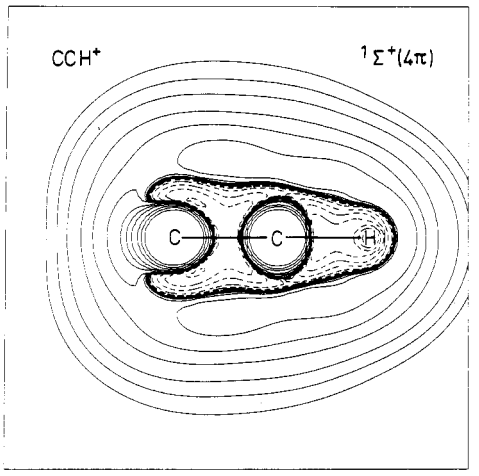

ⓐ

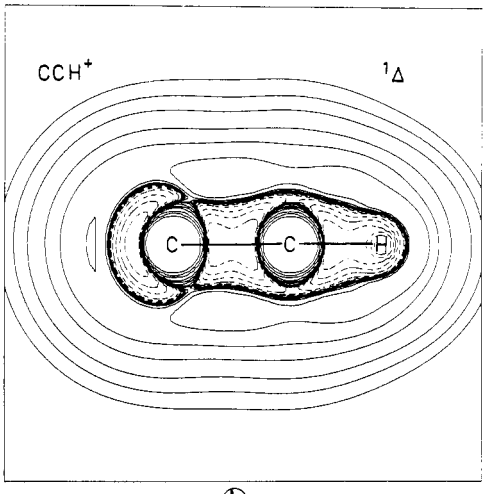

ⓑ

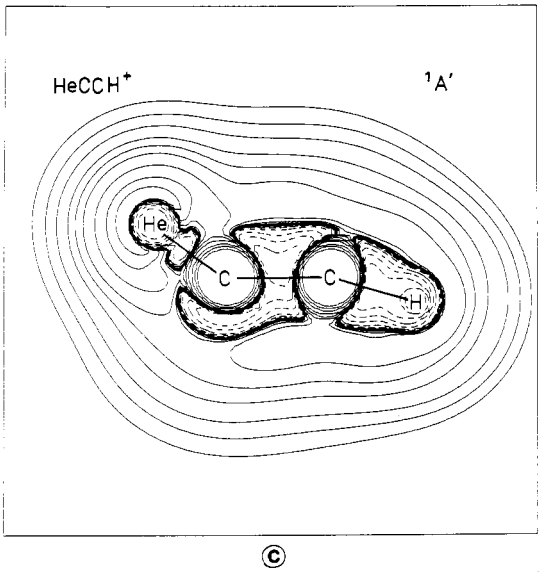

ⓒ

Figure 14. Contour line diagrams of the Laplace concentration $-\nabla^2\rho(\mathbf{r})$ of (a) CCH^+, $^1\Sigma^+(4\pi)$, (b) CCH^+, $^1\Delta$, and (c) $HeCCH^+$ (**14b**). See also caption of Figure 2.

We investigated **15**, **16**, and **17** at all levels of theory employed in our study. All three neutral structures were calculated with rather short He–C and He–B atomic distances (Chart I), although the He–C distance in **16** is longer compared to **8a**, **10a**, **11**, and **14** but shorter than in **10c** and **10e**. The He–B distance in **15** and **17** may be compared with the standard value for a B–H bond (1.21 Å).[67] Inspection of the diagonalized force-constant matrix showed one degenerate negative eigenvalue for **15** and **16** at all levels of theory employed in this study corresponding to imaginary frequencies with π symmetry. Geometry optimization without linear constraints resulted in dissociation. This means that structures **15** and **16** are not minima on the respective potential energy hypersurface.

Scheme IV. Calculated Reaction Energies for He Dissociation of Structures **17b** and **19** at MP4(SDTQ)/6-311G(2df,2pd)//MP2/6-31G(d,p) + ZPE + BSSE

HeBCH (**17b**) → He + HCB(^{1}A′,2π) −5.7 kcal/mol (19)

HeBeO (**19**) → He + BeO($^1\Sigma^+$) +3.0 (+3.5)[a] kcal/mol (20)

[a] CASSCF result (see text).

In contrast to this, linear HeBCH (**17a**) has only positive eigenvalues of the hessian matrix at the Hartree–Fock (3-21G and 6-31G(d,p)) level of theory. As for $HeCCH^+$, the linear structure **17a** was not a minimum at MP2/6-31G(d,p), but a trans bent geometry **17b** was found 2.8 kcal/mol lower in energy than **17a** with only positive eigenvalues of the hessian matrix. Thus, HeBCH is predicted to be a true minimum on the potential energy surface at the MP2/6-31G(d,p) level of theory. The calculated atomic distance for He-B (1.282 Å) is only slightly longer than a standard B–H bond (1.21 Å).[67]

Is HeBCH a stable molecule? Helium dissociation of **17b** yields HCB. A previous investigation[68] predicts that the lowest lying singlet state of HCB at the HF/6-31G(d,p) level is a quasi-linear ^{1}A′ state. We found that inclusion of correlation energy in the geometry optimization yields two ^{1}A′ states which are the result of Renner distortion[57] of the $^1\Delta$ state, both being lower in energy than the $^1\Delta$ state. The lower lying state has ^{1}A′ symmetry with two π electrons and has a strongly bent geometry with a H–C–B angle of 74.2° (Table III). The calculated dissociation reaction of **17b** in HCB (^{1}A′(2π)) and He (reaction 19, Scheme IV) shows that at higher levels of theory HeBCH is no longer stable. While at MP2/6-31G(d,p) the dissociation reaction 19 is endoenergetic by 0.4 kcal/mol, it becomes exoenergetic by −1.8 kcal/mol at MP4(SDTQ)/6-311G(2df,2pd). Correction by ZPE and BSSE[69] increases this to −5.7 kcal/mol. Thus, HeBCH is predicted not to be a stable molecule.

The significant decrease in the bond strength of the He–C bond in going from the dications to the monocations shows that the Coulomb attraction strongly enhances the attracting interaction of an acceptor with helium. In neutral molecules the polarizing power of the charge is absent. However, polarization of helium might be achieved if the acceptor molecule has a dipole moment and helium is attached to the electron deficient center. This explains why HeBCH (**17**) is much lower in energy compared to the isomeric structure HeCBH (**16**) (Table I). Further increase of the polarity of the acceptor molecule should therefore enhance the prospect of finding a helium bond in a neutral compound.

Suitable candidates are HeBN (**18**) and HeBeO (**19**). Both were found to be true minima at the 6-31G(d,p) level. At MP2/6-31G(d,p), HeBN (**18**) dissociates into He and BN. In contrast to the other neutral structures **15**–**18**, HeBeO (**19**) was found to be a stable molecule at all levels of theory employed in our study. Dissociation of HeBeO (**19**) yields He and BeO (reaction 20) which is known to have a $^1\Sigma^+$ ground state.[70,71] At MP2/6-31G(d,p), reaction 20 is endoenergetic by +4.7 kcal/mol. At MP4(SDTQ)/6-311G(2df,2pd) a value of +4.6 kcal/mol is

(67) *Tables of Interatomic Distances and Configuration in Molecules and Ions*; The Chemical Society: London, 1958; Special Publication no. 11.
(68) Luke, B. T.; Pople, J. A.; Schleyer, P. v. R. *Chem. Phys. Lett.* **1985**, *122*, 19.
(69) The total energy of He at MP4(SDTQ)/6-311G(2df,2pd) using the basis set of HeBCH and HeBeO at their MP2/6-31G(d,p) optimized geometry is 0.3 and 0.2 kcal/mol lower, respectively, compared with the calculated energy for isolated He.
(70) Huber, K. P.; Herzberg, G. *Molecular Spectra and Molecular Structure—Constants of Diatomic Molecules*; Van Nostrand Reinhold: New York, 1979.
(71) (a) Schaefer, H. F., III *J. Chem. Phys.* **1971**, *55*, 176. (b) Schaefer, H. F., III *Ibid.* **1972**, *56*, 3938.

Chart II. Calculated Energies [hartrees] and Bond Distances [Å] for HeBeO and BeO at the CASSCF Level

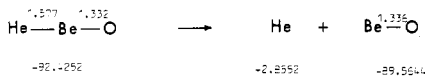

predicted, which lowers to +3.0 kcal/mol after correction for ZPE and BSSE.[69] Three degrees of translational freedom and 1 mol of helium are gained in reaction 20. This gives rise to $+^3/_2\,RT$ (0.9 kcal/mol) for the translational energy correction and $+1\,RT$ (0.6 kcal/mol) for the work term (see eq I). The temperature correction for the vibrational degrees of freedom is estimated as −0.8 kcal/mol.[38] This leads to a predicted dissociation enthalpy for reaction 20 of +3.7 kcal/mol.

To ensure that our results, based on a monoconfiguration method, are not an artifact of the method used, we performed MCSCF calculations as described in the method section employing the program GAMESS.[37] The calculated data are exhibited in Chart II.

By using the CASSCF total energies the dissociation reaction of HeBeO (reaction 20) is predicted to be endoenergetic by +3.5 kcal/mol, in good agreement with the predicted value of +4.4 kcal/mol at MP4(SDTQ)/6-311G(2df,2pd) + BSSE. The He–Be distance is slightly longer at the CASSCF level compared to the MP2/6-31G(d,p) result, while the Be–O distance is shorter and nearly the same compared to isolated BeO (Chart II). Also the MP2/6-31G(d,p) results predict that the Be–O distance should become slightly shorter as the result of He–Be bond formation (Chart I and Table III). Since helium can only act as an electron donor, a slightly positive charge is predicted for He in **19** by the Mulliken population analysis (Chart I).

The Laplace concentration of BeO (Figure 15a) suggests that Be has lost its valence shell electrons to oxygen and thus is essentially ionic with Be^{2+} serving as electron acceptor for He. However, no semipolar bond is established between He and Be. The He–Be interaction is rather characterized as closed-shell interaction with hardly any deformation of the electron structure of BeO and He. This is obvious from Figure 15b and the calculated H_b value for the HeBe bond (Table V).

The electronic structure of BeO in its $^1\Sigma^+$ ground state is schematically shown in Figure 12. Orbital interaction with He is possible via the 5σ LUMO. Since BeO has 4π electrons, bending of HeBeO is energetically unfavorable. Although the 5σ orbital is significantly higher lying than the LUMO of CC^{2+} ($^1\Sigma^+_g$), it is still sufficiently low to have stabilizing interaction with helium which amounts to ~4 kcal/mol. Since Be is the electron deficient center of BeO, HeBeO is formed and not HeOBe.

Why does BN not form a stable HeBN ground state? BN is isoelectronic with BeO, and the LUMO of BN at HF/6-31G(d,p) is even slightly lower (−2.45 eV) compared with BeO (−1.25 eV). In fact, at the HF/6-31G(d,p) SCF level HeBN is calculated to be more strongly bound (8.5 kcal/mol) compared with HeBeO (4.2 kcal/mol). However, correlation contributions are unfavorable for HeBN which has the next unoccupied σ orbitals much higher lying (15.3 and 8.6 eV) than BeO (10.7 and 6.5 eV).

The question if a neutral species is capable of attracting helium sufficiently to form a weak bond seems to be a delicate balance among orbital levels, electron density of the acceptor atom, and dipole moment inducing a dipole–dipole interaction. In the isoelectronic series BN, BeO, LiF only BeO has computationally been found to form a minimum structure with He. HeLiF dissociates at the HF/6-31G(d,p) as well as MP2/6-31G(d,p) level of theory. Also MgO, valence isoelectronic with BeO, was found not to bind He.

4. Chemical Significance

The results of this study should not simply be considered as an exotic extension of our knowledge of chemical bonding which is of purely theoretical interest. Helium is the second most abundant element in interstellar space.[51] Interstellar reactions are often ionic, and He^+ is known to be an important reactant in charge exchange reactions.[51,72] He^+ is produced by direct-ray ionization and destroyed mainly by reaction with CO.[51,72] The library of chemical reactions for gas-phase chemistry in interstellar clouds lists no less than 80 charge exchange reactions involving He^+, and many processes in the ion-molecule chemistry of dark clouds are only comprehensible by the participation of helium cation.[51,73] More than 80 molecules have been identified in interstellar space, and several of them are cations.[51,72] Our result that helium may be strongly bound in charged species suggests that He molecules could play a role in chemical processes in outer space, if only as shortlife intermediates. Since a helium–carbon ion has been observed in a helium–carbon discharge process using graphite,[30] it is conceivable that similar processes might occur on grain surfaces in outer space. Experimental results point to the presence of graphite or some other carbonaceous solid as a major component of interstellar dust.[51] We are currently exploring the stability of helium-containing cations which are of potential interstellar interest.

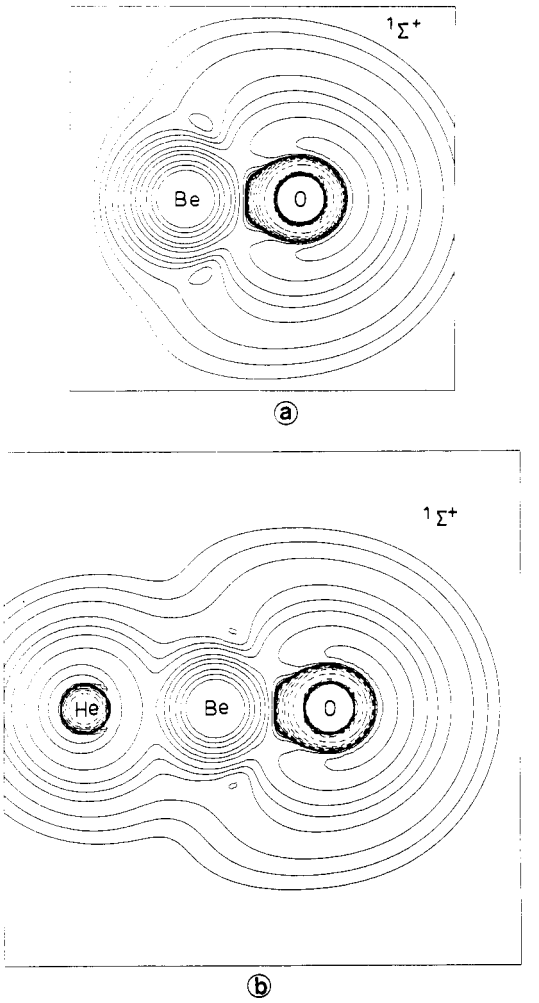

Figure 15. Contour line diagrams of the Laplace concentration $-\nabla^2\rho(\mathbf{r})$ of (a) BeO and (b) HeBe O (**19**). See also caption of Figure 2.

Besides the field of interstellar chemistry, our results on helium chemistry lead to improved knowledge of chemical bonding and show that compounds should be observable which may have never been searched for. HeBeO is the first example of a neutral molecule containing helium which is predicted to be stable. Fluid and solid noble gases are used extensively as a means for trapping instable or very reactive molecules and intermediates to allow the investigation of isolated species. Preliminary investigations have shown that neon also is capable of forming strong bonds to electron deficient atoms and molecules.[74] In the light of our investigations

(72) (a) Herbst, E.; Klemperer, W. *Astrophys. J.* **1973**, *185*, 505. (b) Dalgarno, A.; Black, J. H. *Rep. Prog. Phys.* **1976**, *39*, 573.
(73) Prasad, S. S.; Huntress, W. T. *Astrophys. J.* **1980**, *43S*, 1.
(74) Frenking, G., to be published.

some caution is suggested in the interpretation of results based on trapping experiments with use of noble gases as "inert" media since the observed species may be rather weakly bound noble gas compounds. For example, Brom and Weltner[76] reported the ESR spectrum of $^2\Sigma$ BeOH in an argon matrix and found an anomalously low value for the parallel g tensor. They concluded that this result was "...difficult to explain theoretically, but it could arise from matrix effects".[76] This "matrix effect" might be that the measured species was a weakly bound ArBeOH molecule rather than BeOH.

What is the prospect of examining our results experimentally? Inspired by our predictions[1b] Young and Coggiola[30] recently detected an ion in a mass spectrometer containing a carbon–helium bond formed by interaction of He^+ with graphite. However, this is not a very selective way, and the method may be of limited use. A more promising route could be via tritiated compounds as precursors. β-decay of tritium yields $^3He^+$, and the comparatively short lifetime of tritium (ca. 12.5 years[28b]) secures a sufficient yield of He ions from the respective precursors via reaction 21.

$$RT \rightarrow RHe^+ + \beta^- + n \qquad (21)$$

Reaction 21 has been studied for many tritiated hydrocarbons[28] but mainly for investigation of the carbenium ions which result when helium dissociates from RHe^+ yielding R^+. Mass spectrometric analysis of the relative abundances of the ionic fragments of various tritiated hydrocarbons revealed only spurious amounts of He cations.[28,29] However, the investigated molecules so far are not very promising candidates to detect helium cations with significant yield. For example, CH_3T gives only 0.6 ± 0.01% CH_3He^+.[29] It can easily be predicted from our results that CH_3He^+ should have a very weak He–C bond. In fact, Wong et al.[19] calculated that the He–C atomic distance in CH_3He^+ is only 2.053 Å, and the barrier for dissociation is predicted to be less than 0.3 kcal/mol. Our results suggest that tritiated acetylene, HCCT, is a much better candidate as precursor for a helium ion. β-decay of HCCT gives $HeCCH^+$ (**14b**) which is predicted to be stable toward He loss giving singlet CCH^+.

$$TCCH \rightarrow HeCCH^+ \text{ (14b)} + \beta^- + n \qquad (22)$$

Unless an intersystem crossing occurs to the more stable triplet states[64] of CCH^+, which is unlikely for such a small molecule, $HeCCH^+$ should be observable as significant product of HCCT via reaction 22. This would make a helium ion available which can be used in gas-phase ion reactions.

What about HeBeO? The problem here is to make monomeric BeO which should immediately give HeBeO in fluid or solid helium. BeO is a polymeric solid[75] but monomerizes at high temperature. Experimentally this seems not to be an unsolvable problem. More difficult might be the identification of HeBeO. While the MP2/6-31G(d,p) data predict a frequency shift of the Be–O vibration of ca. 100 cm^{-1}, the CASSCF results show that the BeO distance should nearly be the same in HeBeO and in the isolated molecule. However, two new frequencies with low vibrational numbers should appear as the result of bond formation in HeBeO, and a sensitive IR measurement should be able to detect and identify HeBeO by the occurrence of these two vibrations.

5. Conclusion and Outlook

Helium can form strong chemical bonds in ions and may even be bound in the ground state of a neutral molecule. The electronic structure of a potential acceptor atom or molecule is of crucial importance for the bond strength to helium. The helium bond can be very strong if an acceptor provides low-lying empty σ orbitals. Helium may donate significant electronic charge into σ orbitals of binding partners to which it is bound, and a potential binding fragment must provide empty or half empty low-lying σ orbitals (σ-holes) in order to form a strong chemical bond to helium. The He–C bond strength in dications can be in the order of 90 kcal/mol, and in monocations it can be 30 kcal/mol. The bond strength is markedly reduced in neutral molecules compared to cationic species. The features of helium compounds can be rationalized as donor–acceptor compounds between He as electron donor and the respective acceptor fragment. This explains the differences encountered when isoelectronic helium and hydrogen compounds are compared.[77]

The principal feature for binding helium revealed in our investigation does not exclude similar binding in heavier noble gases such as neon. Although neon has completely filled 2p orbitals which will produce net repulsion when interacting with other filled π orbitals, Ne might donate electrons into empty π orbitals, and the 2s orbital of Ne is energetically higher lying than the 1s orbital of He. In addition, neon is more polarizable than helium. We have already performed first calculations of neon-containing cations and neutral compounds and found the bond dissociation energies in analogue compounds to be similar to helium compounds.[74]

The possible existence of helium-containing ions has been predicted in several theoretical investigations before.[16-27] The results reported here are based on more extensive calculations than all previous studies and allow a reliable prediction concerning the stability of the investigated compounds. Furthermore, the analysis of the electronic structure of He compounds suggests a donor–acceptor model which allows one to predict qualitatively if a molecule containing helium might possibly exist. Several He compounds are predicted by this investigation to be stable or metastable. Our results are a challenge for experiment!

Acknowledgment. G.F. thanks Dr. Brian T. Luke for many helpful comments and discussions. W.K. thanks Dr. Nikolaus Heinrich for stimulating discussions. We are indebted to Prof. Leo Radom for sending a manuscript prior to publication and to Prof. Paul v. R. Schleyer for pointing out his calculations of ions containing light noble gas elements. Stimulating comments by Prof. Christian K. Jørgensen, Prof. Joel F. Liebman, and Prof. William Klemperer are gratefully acknowledged. Calculations have been carried out at the computation centers of the TU Berlin and the Universität Köln. Part of this work has been supported by the Deutsche Forschungsgemeinschaft and the Fonds der Chemischen Industrie.

Registry No. 1, 106007-05-0; **2**, 106007-04-9; **3**, 105554-33-4; **4**, 12269-21-5; **5**, 11092-10-7; **6**, 53262-54-7; **7**, 53262-53-6; **8**, 108673-00-3; **10**, 109909-09-3; **11**, 109909-10-6; **12**, 109909-11-7; **13**, 109909-12-8; **14**, 80909-47-3; **15**, 109909-13-9; **16**, 109909-14-0; BCH, 56125-76-9; BN, 10043-11-5; BeO, 1304-56-9; He, 7440-59-7.

Supplementary Material Available: Representative molecular orbital calculations using GAUSSIAN82, GAMESS, and COLOGNE (6 pages). Ordering information is given on any current masthead page.

(75) Cotton, F. A.; Wilkinson, G. *Anorganische Chemie*, 4th ed.; Verlag Chemie: Weinheim, 1982; p 280.

(76) Brom, J. M., Jr.; Weltner, W., Jr. *J. Chem. Phys.* **1976**, *64*, 3894.

(77) A systematic comparison of isoelectronic hydrogen and helium compounds is presented by the following: Frenking, G.; Koch, W.; Liebman, J. F. In *Molecular Structure and Energetics*; Greenberg, A., Liebman, J. F., Eds.; VCH Publishers: Deerfield, FL, Vol. 8, in press.